Development of 3D Advanced Rapid Prototyping Multipurpose Structures with Micro and Nano Materials

F. Mancia*, M. Marchetti, M. Regi**, S. Lionetti***
A. Marranzini, F. Mazza**, P. Coluzzi****

* C.S.M. Centro Sviluppo Materiali S.p.A.
Via di Castel Romano 100, 00128 Roma

** University of Rome "La Sapienza", Department of Aeronautics and Astronautics Engineering
Via Eudossiana 18, 00184 Roma

f.mancia@c-s-m.it; mario.marchetti@uniroma1.it; marco.regi@uniroma1.it

ABSTRACT

In various areas of manufacturing, research and education, the 3D rapid prototyping methods are widely employed. Typical applications are engineering, architecture, medicine. The present technical and commercial demand requires the development of faster and cheaper methodologies for structures design and realization. Different techniques, based on CAD platforms and Rapid Prototyping (RP) are available.
The conceptual steps of the design are: theoretical and FEM analysis, virtual 3D CAD model, RP shape processing.
The RP method allows to produce also simulacra (demonstrators and prototypes) useful to analyze the characteristic of a complex system (ex. interference between the dynamic parts, cinematic behavior, geometric evaluation, quality and reliability).
The RP elements produced normally are moulds (for metal casting but also for RTM (Resin Transfer Molding) process of polymeric composite materials) or mandrel for Filament Windings processes.
The limits of the RP are the time requested by the process and the limited volume of the samples producible.
The target of the present work is the development of an automatic RP procedure, useful to produce high quality and complex geometry components, characterized by high material yield, significant reduction in the manufacturing time and low final cost.
In particular, the Authors discuss the innovative realization of advanced lattice multigrid structures for aerospace applications, made of polymeric composite materials (PCM) and of metallic alloys.
The properties of prototyped samples and structures are evaluated by mechanical test (static and dynamic).

PCM lattice structures were realized by Filament Winding (FW) on a negative mould (mandrel) produced by Stereo Lithography (SLA). A numerical model of the RP curing phase is discussed.
The use of micro and nanostructured polymeric composite materials is moreover illustrated. The addition of nano – particles gave an improvement of mechanical properties.

Metallic structures were directly realized by Laser Sintering. The metallic powders employed are characterized by the SEM and with a statistical analysis (SIA – Software Imagine Analysis) of the dimension and shape. These parameters have direct influence on the manufacturing feasibility and final performance of the component.

Mancia, F.; Marchetti, M.; Regi, M.; Lionetti, S.; Marranzini, A.; Mazza, F.; Coluzzi, P. (2006) Development of 3D Advanced Rapid Prototyping Multipurpose Structures with Micro and Nano Materials. In *Cost Effective Manufacture via Net-Shape Processing* (pp. 20-1 – 20-24). Meeting Proceedings RTO-MP-AVT-139, Paper 20. Neuilly-sur-Seine, France: RTO. Available from: http://www.rto.nato.int/abstracts.asp.

Report Documentation Page

Form Approved
OMB No. 0704-0188

1. REPORT DATE	2. REPORT TYPE	3. DATES COVERED
MAY 2006	**N/A**	**-**

4. TITLE AND SUBTITLE	5a. CONTRACT NUMBER
Development of 3D Advanced Rapid Prototyping Multipurpose Structures with Micro and Nano Materials	5b. GRANT NUMBER
	5c. PROGRAM ELEMENT NUMBER
6. AUTHOR(S)	5d. PROJECT NUMBER
	5e. TASK NUMBER
	5f. WORK UNIT NUMBER
7. PERFORMING ORGANIZATION NAME(S) AND ADDRESS(ES) **C.S.M. Centro Sviluppo Materiali S.p.A. Via di Castel Romano 100, 00128 Roma**	8. PERFORMING ORGANIZATION REPORT NUMBER
9. SPONSORING/MONITORING AGENCY NAME(S) AND ADDRESS(ES)	10. SPONSOR/MONITOR'S ACRONYM(S)
	11. SPONSOR/MONITOR'S REPORT NUMBER(S)

12. DISTRIBUTION/AVAILABILITY STATEMENT
Approved for public release, distribution unlimited

13. SUPPLEMENTARY NOTES
See also ADM202748. Cost Effective Manufacture via Net Shape Processing (Rentabilite de fabrication par un traitement de finition immediate), The original document contains color images.

14. ABSTRACT

15. SUBJECT TERMS

16. SECURITY CLASSIFICATION OF:			17. LIMITATION OF ABSTRACT	18. NUMBER OF PAGES	19a. NAME OF RESPONSIBLE PERSON
a. REPORT	b. ABSTRACT	c. THIS PAGE			
unclassified	**unclassified**	**unclassified**	**UU**	**43**	

1.0 INTRODUCTION [1]÷[11]

The actual trend in manufacturing industry is to short the product development cycle using Rapid Prototyping (*RP*) processes. The basic idea is to produce components or parts by using *RP* tools (*RT*) to obtain a tangible prototype of a future product. Such tools are of two types: soft tooling and hard tooling. The first is associated with low volume production and low hardness materials, instead the second is associated with high volume production and hard materials.
The term "*Net Shape*" refers to the original shape of the model in all aspects and details. The term "*Net Shape process*" refers to those methods that are able to produce a model in its final shape without furthers workings, resulting in a partially costs reduction. The term "*Near Net Shape Methods*" is referred to processes demanding small final workings.
There are several manufacturing processes that are classified under the name "*Net Shape Methods*", for example:

- Stereo lithography (*SLA*)
- Fused Deposition Modelling (*FDM*)
- Laminated Object Manufacturing (*LOM*)
- Solid Ground Curing
- Selective Laser Sintering (*SLS*)
- Three – dimensional Printing (*3D Printing*)
- Ballistic Particle Manufacturing (*BPM*)
- Recursive Mask and Deposit (*MD*)
- Laser Assisted Net Shaping process (*LENS Process*)
- Shape Deposition Manufacturing
- Metal Injection Moulding (*MIM*)
- Sheet Metal Forming
- Spray Deposition.

Among these, the most diffuse processes are:

Stereo Lithography (*SLA*) – U.V. laser is used to create successive sections of three-dimensional object within a bath of liquid photopolymer. When the laser passes through the polymer, it hardens; then a platform is moved just below the free surface of the resin. As the laser traces the layer, the resin begins to cure solidifying the part of the object. The Stereo lithographic process can take few minutes per layer, hence it is not a quick process.

Selective Laser Sintering (*SLS*) – Laser light is used to synthesize thin layers of heat-fusible metal powder. The laser beam traces the cross-section of the layer on the surface and the sintering occurs of the portion of powder exposed to laser beam. The material's selection is an important variable under evaluation, because the final product may exhibit warping and shrinkage, strongly dependent on the geometry of the model.

Metal Injection Moulding (*MIM*) – It is a *Net Shape* manufacturing process of complex components. Good mechanical properties of high-performance metallic alloys can be obtained, with very low production's cost. Typical materials for *MIM* are: Tungsten heavy alloy like *W – Ni - Fe* and *W – Ni - Cu*, Carbide, Stainless Steel, Nickel – Copper, Titanium, Carbonitride, Tungsten – Copper.

3D Printing (*3D Printing*) – The process is based on powder solid free form in which a liquid binder is sprayed onto a layer of powder and a pattern is traced. After drying, the process is repeated. When the overall process is finished, the part is heat treated to enhance the bonding of the glued powder.

The methods described can produce structures and elements characterized by very complex shape, according to the "*Net Shape*" concept. Time, costs and quality represent the principal parameters to be evaluated.
This paper shows complex structures by means of Stereo Lithography (polymeric) and direct laser sintering (metallic alloys). Technology assessment of prototypes production and final mechanical behavior are discussed.

2.0 RP MANUFACTURING OF MULTIGRID AEROSPACE STRUCTURES [12]÷[16]

2.1 Rapid Prototyping of the negative moulds

By Stereo Lithography it is possible to produce advanced aerospace structures (ex. multigrid lattice), using the following procedure:

- structure design (theoretical, numerical and FEM)
- 3D CAD drawing of the element (fig. 2.1.1)
- Rapid Prototyping of the positive mould (fig. 2.1.2)
- manufacturing of the negative mould (fig. 2.1.3) by silicone
- manufacturing of the structure (using different techniques as for example filament winding, hand lay up, etc.).

The use of silicone for negative mould allows to obtain the following advantages:

- the mould is cheaper and reusable
- high thermal, chemical and geometrical stability
- feasibility of structural elements of high complex geometry (cylindrical, flat, conics).

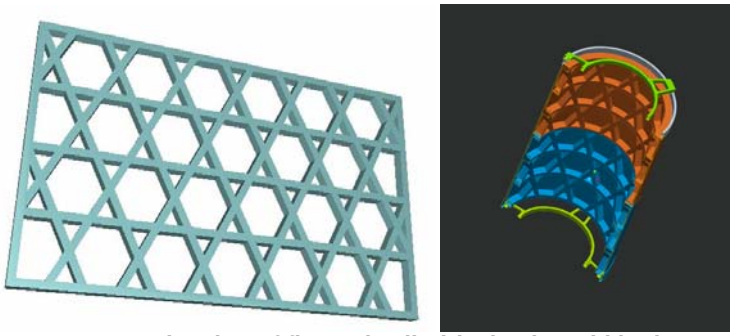

Figure 2.1.1: 3D CAD drawing of flat and cylindrical anisogrid lattice structure

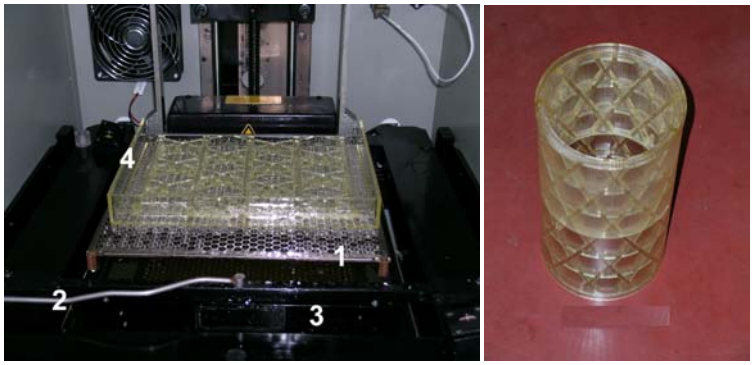

Figure 2.1.2: rapid prototyping of the positive moulds (flat and cylindrical)

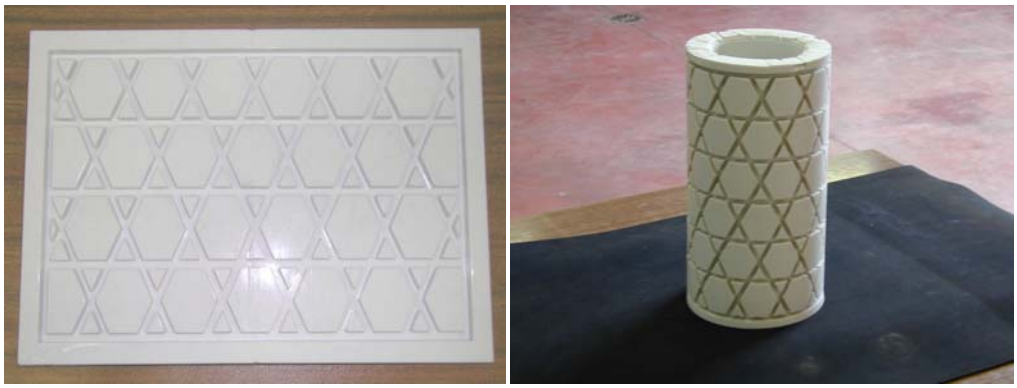

Figure 2.1.3: negative silicone moulds of the structures

By this method it is possible to obtain a significant control of the structure geometry. Figures 2.1.4÷2.1.9, show applications of the negative silicone moulds characterized by geometries of different complexity.

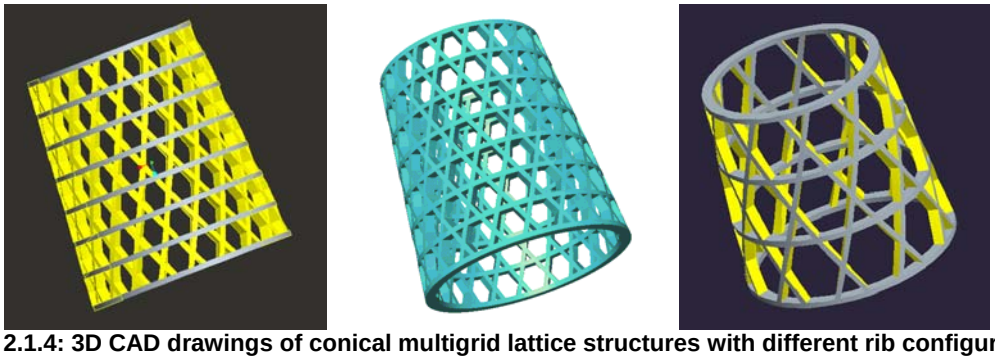

Figure 2.1.4: 3D CAD drawings of conical multigrid lattice structures with different rib configurations

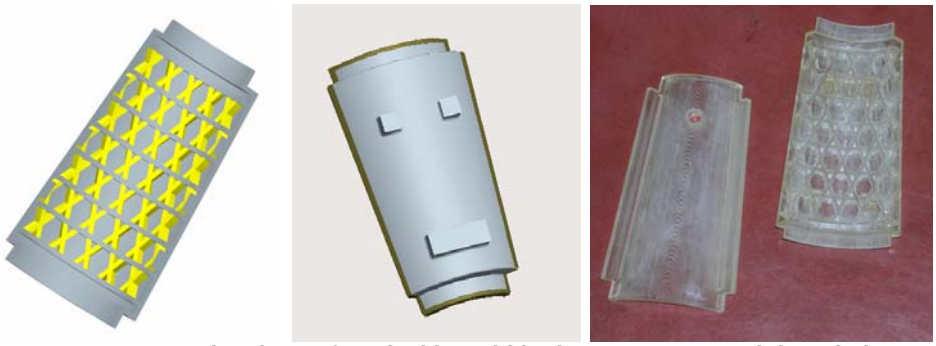

Figure 2.1.5: 3D CAD drawings of conical isogrid lattice structures and the relative rapid prototyped negative moulds

Figure 2.1.6: other view of the conical positive moulds

Figure 2.1.7: positive and negative moulds of the conical anisogrid lattice structure prototype

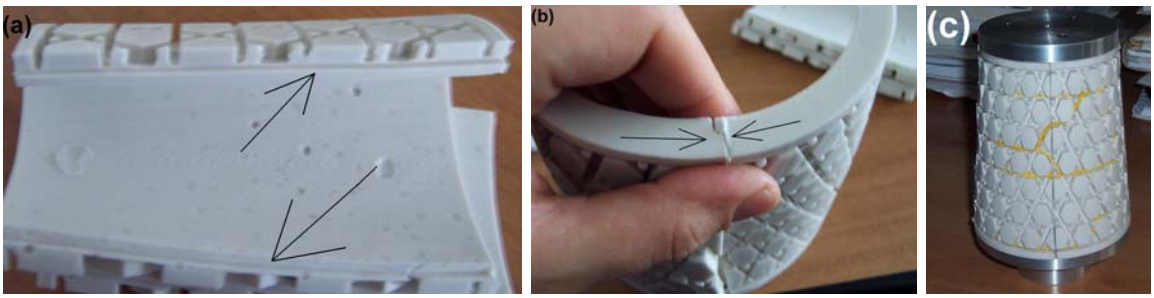

Figure 2.1.8: the assembly and the relative metallic mandrel of the negative silicone conical mould

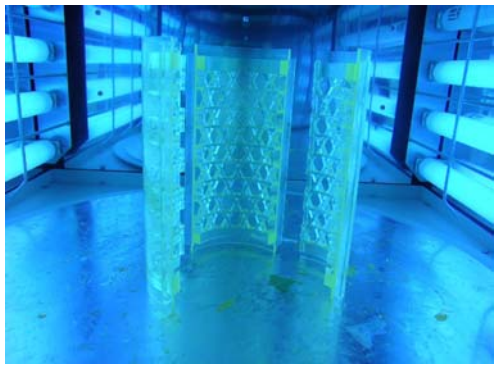

Figure 2.1.9: U.V. treatment of the rapid prototyped positive moulds for a complete curing of the polymer

2.2 Manufacturing of multigrid lattice aerospace structures by FW

The manufacturing of the multigrid lattice structures is characterized by the use of the negative glanularity mould described to the previous paragraph. Filament Winding (FW) of pre – preg glass fibers was utilized. The multigrid complex geometry requires the development of specific fiber sequence depositions. This fundamental to obtain a prototypes mechanical behaviors similar to the those predicted by theoretical, numerical and FEM models.
Fig. 2.2.1 shows the FEM analysis of the flat and cylindrical elements (anisogrid configuration).

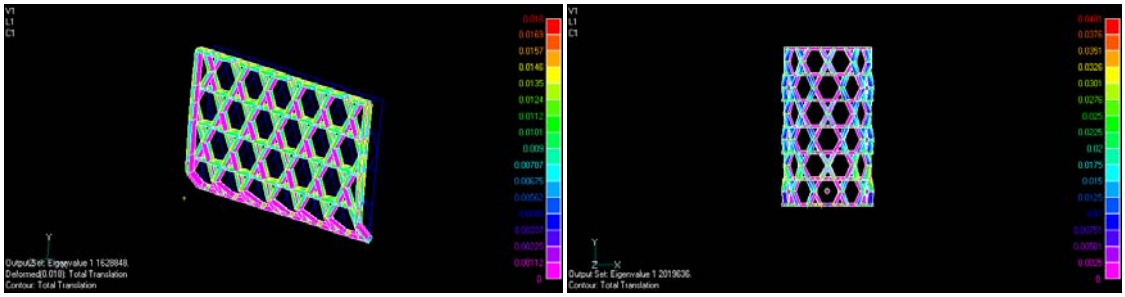

Figure 2.2.1: FEM analysis of the flat and cylindrical anisogrid lattice structures

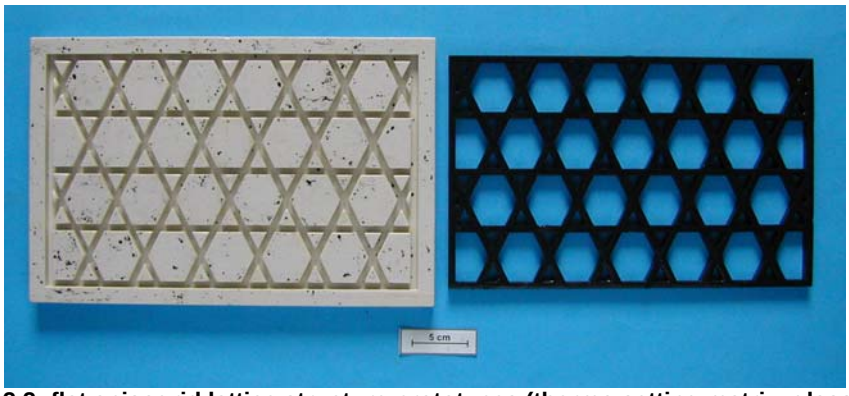

Figure 2.2.2: flat anisogrid lattice structure prototypes (thermo setting matrix, glass fibers and micro and nanoparticles of graphite embedded in the matrix)

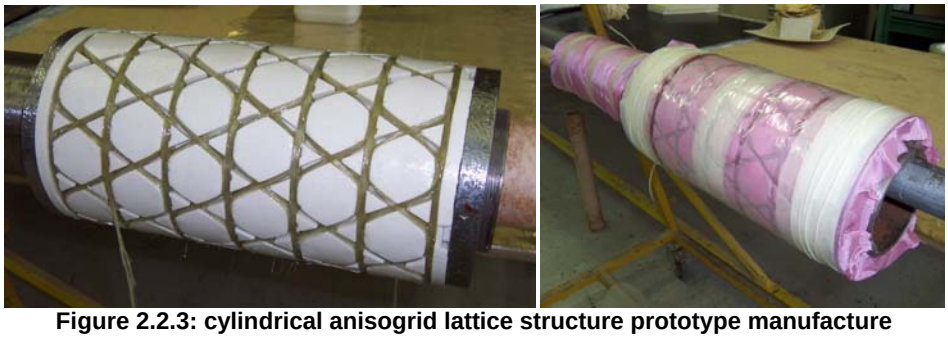

Figure 2.2.3: cylindrical anisogrid lattice structure prototype manufacture

The dimensions of the flat and cylindrical anisogrid lattice structure prototypes are respectively:

- flat element: 330 mm x 265 mm; section: 10 mm x 6 mm
- cylindrical element: height: 300 mm, medium diameter: 160 mm; section: 10 mm x 6 mm.

Figures 2.2.2÷2.2.4 illustrate the technological procedure employed to prototypes manufacturing. The realized prototype demonstrates that by the procedure developed it is possible to obtain structures with high quality, respecting the fundamental concept: "*as drawing as built*", i.e., with a significant respect of the original designed structure dimensions.

Figure 2.2.4: cylindrical anisogrid lattice structure prototype manufacture

2.3 Mechanical tests

Mechanical test were performed to evaluate the buckling behavior of these innovative (anisogrid)

structures.
Fig. 2.3.1 show a pictures sequence of a compression load test of the anisogrid lattice prototype.

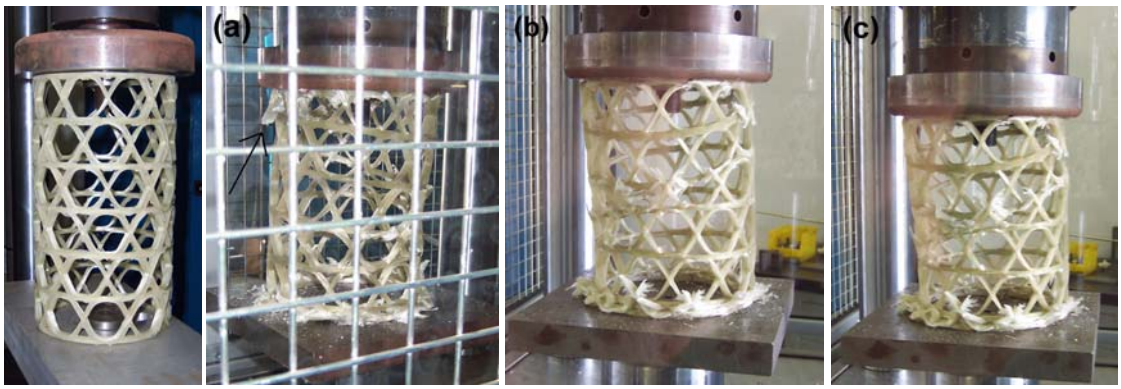

Figure 2.3.1: mechanical behavior of the cylindrical anisogrid lattice structure prototype

The prototypes of fig. 2.2.4 were used. As expected, the experimental results show a differences between the maximized theoretical results and the experimental ones.
The main results of the mechanical test are described in the following points:

- the experimental mechanical behavior of the prototypes is inferior to those predicted (theoretical, numerical and FEM)
- using different fiber deposition sequences the mechanical resistance of the structures changes.

In this case, the major interest it is focalized to the first point, i.e., on the moulds manufacture procedure develop with the rapid prototyping methods.

3.0 DIRECT RP MANUFACTURING OF MICRO AND NANO - STRUCTURED POLYMERIC SAMPLES [12]÷[16]

3.1 Numerical model of Direct RP curing processes

During the direct RP process, a single layer (thickness *h*) of the polymer is cured thanks to the action of a laser spot (wave length λ = 354.7 nm). The properties of the composite produced with this method depends, strongly, by the curing degree (α) of each layer and to the relative chemical bonding between two layers.
α is function of *h*, materials employed (ex. only resin, resin + powders or fibers) and their properties (granularity, density, thermal conductivity, etc), laser parameters (power, spot dimension), initial temperature, time requested to the curing of a single layer, etc.
The target is to obtain a uniform distribution of α in the RP produced elements.
For a numerical evaluation of α, a specific software has been developed. The spot laser act on a single layer (thickness *h*) meshed with *n* nodes (as showed in fig. 3.1.1).

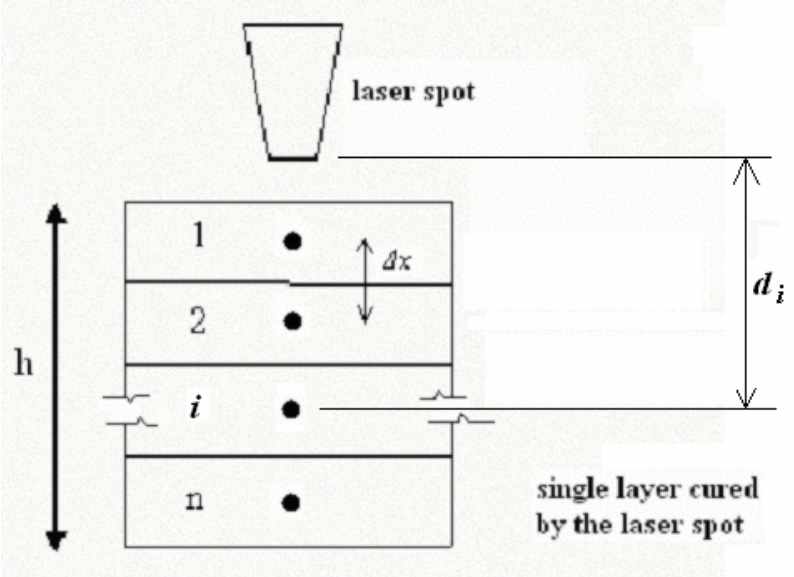

Figure 3.1.1: mesh used for the numerical curing simulation of the single layer polymerized by the laser spot

Using the Arrhenius equation the curing degree ($d\alpha/dt$) of each node (i = 1, 2,……, n) is calculated as a function of the temperature (T). In fact:

$$\alpha_i^{t+1} = \alpha_i^t + (1-\alpha_i^t) A e^{-\frac{E}{RT}} \Delta t \qquad (3.1)$$

The above equation is studied under the following hypothesis:

1. mono – dimensional model
2. conductive heat transfer
3. viscosity negligible.

Considering the dimension *h* and the laser spot diameter (φ), the first hypothesis is realistic. Besides, analyzing the thermal parameter of the materials used, the convective and irradiative heat transfer term is no significant respect the conductivity.
The temperature (T) of the node *i*, calculated respect two different instants (t and t + *1*) and considering

the above hypothesis, can be defined as:

$$T_i^{t+1} = T_i^t\left(1-\frac{2k_{i+1}^t\Delta t}{\left(c_p^t\rho^t\Delta x^2\right)_i}\right)+\frac{k_{i+1}^t\Delta t}{\left(c_p^t\rho^t\Delta x^2\right)_i}T_{i+1}^t+\frac{k_{i-1}^t\Delta t}{\left(c_p^t\rho^t\Delta x^2\right)_i}T_{i-1}^t+\left[\frac{P_{spt}\Delta t}{\left(c_p^t\rho^t\Delta x^2\right)_i A}\right] \qquad (3.2)$$

with:
ρ = density [gr/m^3], c_p = specific heat [J/gr], T = temperature [K], t = time [sec], k = thermal conductivity [W/m K], P = laser power [W], A = area cured by laser spot [mm^2], Δx = mesh size [mm].

Solving equations (3.1) and (3.2) is possible to calculate $\alpha_i = \alpha_i(t)$ (for i = 1, 2,……, n) of the cured layer (h).
The software can to evaluate $\alpha_i = \alpha_i(t)$ in three different operative conditions:

1. only resin
2. resin + fibre
3. resin + powders.

Naturally, with different fibres and powders quantities dispersed in the polymeric matrix. In this case considering the properties (ρ, k, etc.) of the single elements (polymer, fibres or powders), it is possible to determine the equivalent properties of the composite that, during the laser curing process, vary in each instant (t). Besides, case **1.** represent the RP manufacturing of mould and simulacra (see paragraph 2.1, fig. 2.1.9). While **2.** and **3.** simulate the direct RP process studied in the paragraph 3.3.
To validate the software, a numerical simulations has been performed with the parameters reported in tab. 3.1.1. Case **3.** has been analysed, considering a 10% in *wt* of micro particles (graphite) uniformly dispersed in the resin.

Table 3.1.1: parameters used in the numerical simulation of direct RP of micro and nano – structured polymeric composite (see par. 3.3)

n	**Laser power**	***h***	**Laser spot (φ)**	**Initial temperature (T_{in})**	**Resin density**
5	100 mW	0.1 mm	(0.25 ± 0.025) mm	25 °C	1.26E6 gr/m^3
Graphite density	**Resin thermal conductivity**	**Graphite thermal conductivity**	**Resin specific heat**	**Graphite specific heat**	**Graphite percentage**
1.79E6 gr/m^3	0.167 W/m K	1.04 W/m K	1.267 J/ gr K	0.712 J/ gr K	10 % in wt

Fig. 3.1.2 illustrate numerical simulation results (curing degree (α) vs. time (t)) for each node (i) of the single cured layer (h, fig. 3.1.1).

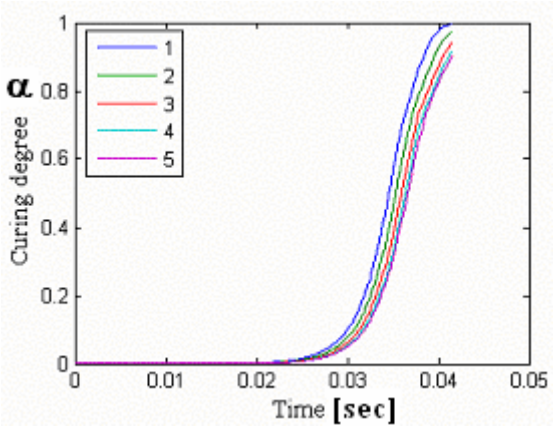

Figure 3.1.2: curing degree (α) vs. time (t, sec) numerical simulation of the single cured layer (h), for each node (i = 1, 2,……, 5)

Fig. 3.1.2. shows that each node (*i*) has a similar curing profile. In particular, it is possible to note that:

- increasing the distance node – laser spot (d_i, fig. 3.1.1), the curing velocity ($d\alpha/dt$) decrease (fig. 3.1.3)
- time requested to reach the final value of α (~ 1) is very rapid (O(E-2) sec). This result is in full agreements with the experimental data.

Besides, has been observed that increasing the initial temperature (T_{in}), $d\alpha/dt$ increase.

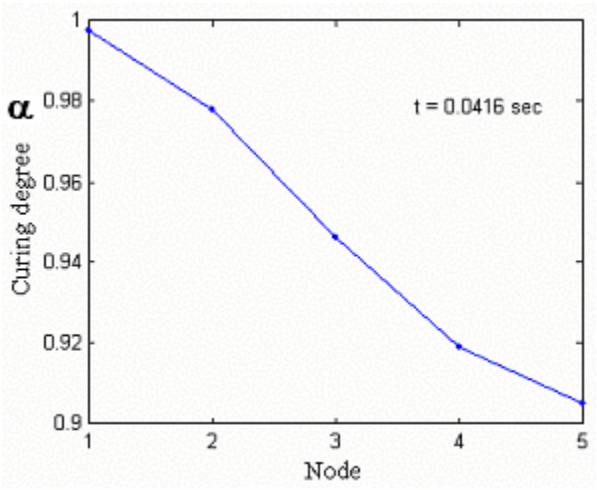

Figure 3.1.3: the curing degree (*α*) of the nodes (*i* = 1, 2,……, 5) calculated at an instant *t*. The curve indicates that increasing the distance d_i (see fig. 3.1.1) *α* is reduced (and then also *dα*/*dt*)

The curing degree (α) profile is asymptotic to the unitary value (fig. 3.1.4). This result (provided by the software) is in full agreement with the Arrhenious theory.

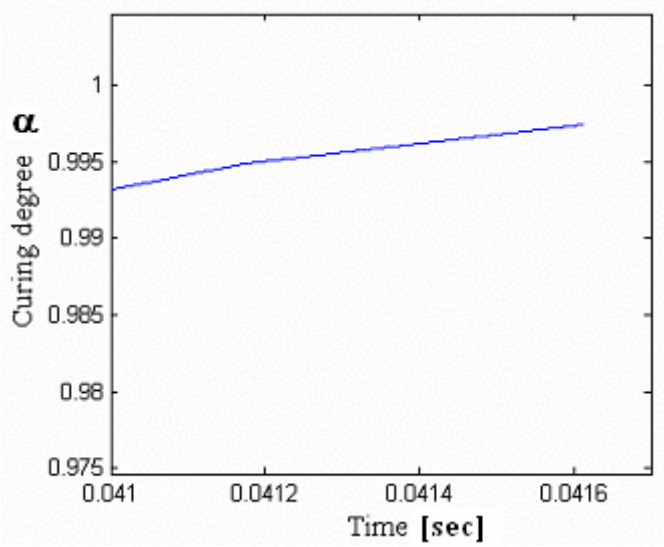

Figure 3.1.4: asymptotic profile of the curing degree (*α*) for each node (*i* = 1, 2,……, 5) of the meshed single layer (*h*) cured by laser

For each node (*i*) of the meshed layer (*h*), the software can to calculate the curing degree (α vs. t) in function of the different quantities of the powders (and/or fibers) dispersed in the matrix. Fig. 3.1.5 shows an example of α vs. t (for i = 5) in correspondence of the different quantities of carbon powders (0 %, 20 %, 40 % in wt) employed. The curves indicates that the curing velocity ($d\alpha/dt$) decrease when the powders

quantity is increased.

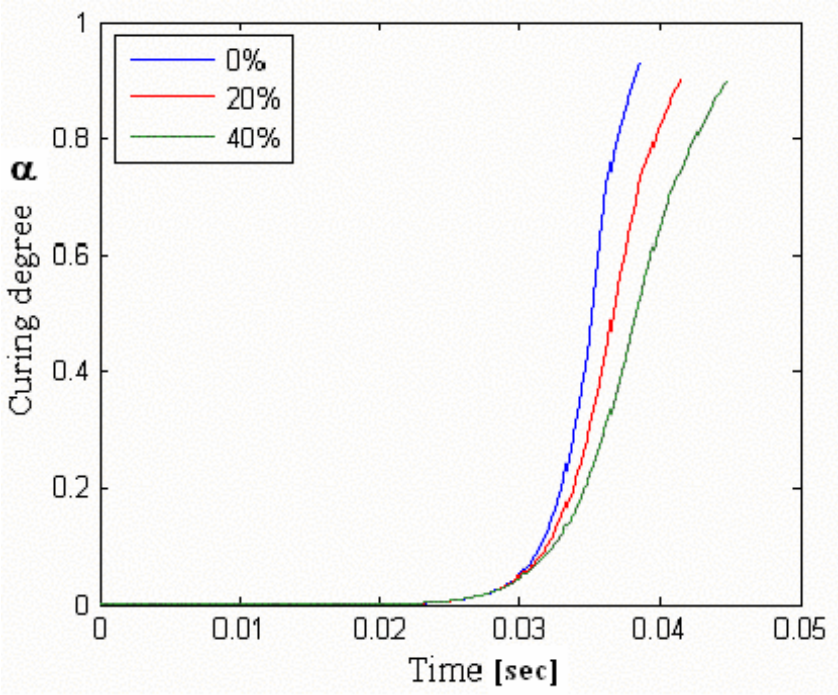

Figure 3.1.5: curing degree (α) vs. time (t) of the node n = 5 using different quantities of the carbon powders dispersed in the polymeric matrix

The software developed represent an important instrument to simulate the direct RP processes of micro and nanostructured polymeric materials (as described in the par. 3.3).

3.2 SEM analysis of the micro - powders added in the polymeric matrix

An important test is the SEM characterization of the particles embedded in the matrix. Using a specific sample preparation procedure (developed by the Authors) the micro carbon particles (graphite) has been observed by the SEM (fig. 3.2.1).

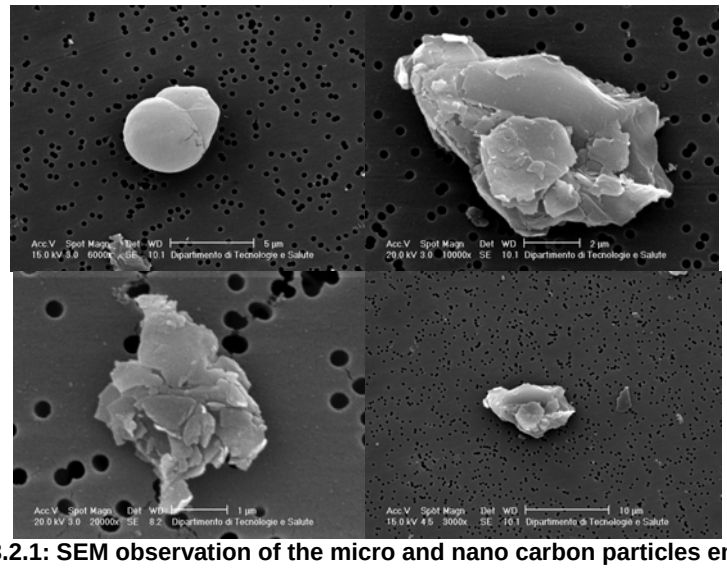

Figure 3.2.1: SEM observation of the micro and nano carbon particles employed in the RP of micro and nanostructured polymeric composite materials

With a specific software integrated in the SEM, a statistic analysis (SIA) of the particles dimension is performed. This typology of analysis is necessary to evaluate the morphology (dimension, geometry, shape) of the particles embedded in the matrix. The software determines a particles groups, each with a specific range of dimension (indicated by different colors in the SEM micrograph reported in fig. 3.2.2). Then, the main particles dimensions (perimeter, area, mean/max/min diameter) are obtainable (tab. 3.2.1).

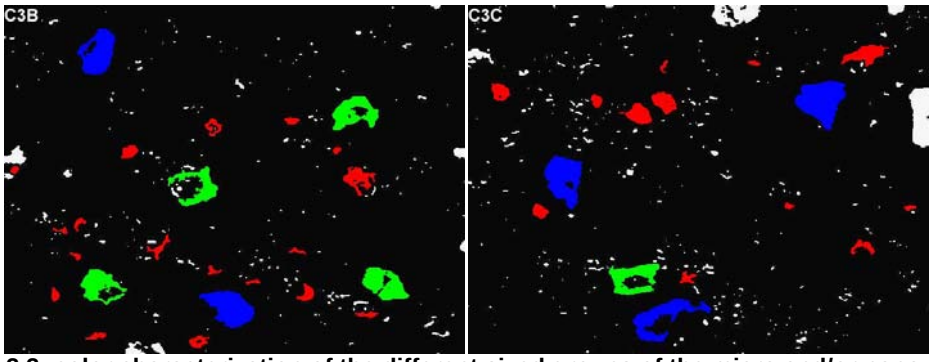

Figure 3.2.2: color characterization of the different sized groups of the micro and/or nano particles observed by SEM (sample n° 1 and n° 2)

Table 3.2.1: SEM statistical analysis of the carbon particles used in the micro and nanostructured polymeric composite materials

	ID Particle	ID Class	Area	Diameter Mean	Diameter Max	Diameter Min	Perimeter
			µm²	µm	µm	µm	µm
SAMPLE n° 1 (fig. 3.2.2 left, ref. C3B)							
	1	3	8,11	3,77	4,25	3,08	15,98
	2	2	6,73	3,83	4,19	3,12	17,71
	3	1	0,60	1,14	1,38	0,65	3,17
	4	1	1,00	1,47	1,53	1,32	7,97
	5	1	1,20	1,42	1,57	1,10	4,25
	6	1	0,32	0,68	0,74	0,61	2,05
	7	1	0,35	0,71	0,78	0,67	2,19
	8	2	5,48	4,08	4,45	3,15	21,60
	9	1	3,22	2,66	2,88	2,36	14,44
	10	1	0,53	1,08	1,16	0,84	3,84
	11	1	0,33	1,15	1,37	0,62	3,47
	12	1	1,07	2,12	2,34	1,53	7,38
	13	1	0,39	1,33	1,57	0,58	3,67
	14	1	0,33	0,92	1,08	0,57	2,68
	15	1	0,42	1,12	1,26	0,75	3,61
	16	2	6,98	3,75	4,42	2,48	16,15
	17	2	6,01	3,58	4,08	2,83	19,00
	18	1	0,33	1,13	1,30	0,53	2,91
	19	1	1,13	1,52	1,59	1,46	5,10
	20	1	0,59	1,09	1,26	0,71	3,13
	21	3	9,10	4,26	5,08	2,99	13,66
	22	1	0,62	1,75	2,05	0,62	4,62
	23	1	0,64	1,59	1,81	0,61	4,09
	24	1	1,10	1,55	1,80	1,12	6,38
mean			**2,36**	**1,99**	**2,25**	**1,43**	**7,88**
max			**9,10**	**4,26**	**5,08**	**3,15**	**21,60**
min			**0,32**	**0,68**	**0,74**	**0,53**	**2,05**

SAMPLE n° 2 (fig. 3.2.2 right, ref. C3C)							
	1	1	3,75	3,61	4,35	1,91	10,87
	2	1	0,32	0,99	1,10	0,75	3,29
	3	1	0,32	0,94	1,14	0,42	2,50
	4	3	11,33	4,42	4,55	4,14	14,48
	5	1	1,73	1,66	1,89	1,39	5,91
	6	1	2,64	2,09	2,47	1,60	6,89
	7	1	0,80	1,09	1,26	0,86	3,41
	8	1	2,75	2,42	2,92	1,67	7,49
	9	3	9,56	4,22	4,90	3,25	15,74
	10	1	0,31	0,76	0,88	0,53	2,31
	11	1	1,18	1,35	1,47	1,03	4,19
	12	1	0,31	0,89	1,06	0,50	2,48
	13	1	1,12	1,86	2,11	1,44	7,25
	14	2	6,54	4,25	4,51	2,94	20,41
	15	1	0,85	1,41	1,59	1,16	5,27
	16	3	8,41	5,97	6,86	3,04	24,61
mean			**3,24**	**2,37**	**2,69**	**1,66**	**8,57**
max			**11,33**	**5,97**	**6,86**	**4,14**	**24,61**
min			**0,31**	**0,76**	**0,88**	**0,42**	**2,31**

The histograms of main characteristic dimensions (using data in the tab. 3.2.1) can be calculated. For example, fig. 3.2.3 shows the statistical distribution of the max diameter of carbon particles. Different distributions of dimension and shape of the particles modify strongly the final mechanical and physical properties, as discussed in the following par. 3.4.

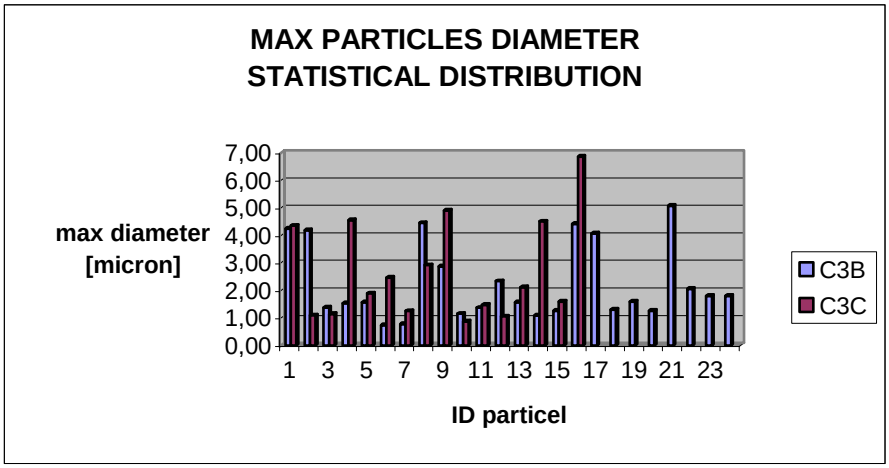

Figure 3.2.3: histogram of the statistical SEM analysis of the max carbon particles diameters (ref. fig. 3.2.2 and tab. 3.2.1)

3.3 Direct Rapid Prototyping of micro and nano – structured polymeric samples

The direct rapid prototyping of the micro and nano - structured polymeric samples requires two preliminary activities:

1. resin degassing
2. evaluation of the decantation and/or deposition time of the micro and nanoparticles embedded in the liquid resin.

The resin degassing (for ~ 24 h) has been performed using a glass chamber in which the vacuum condition are reached (fig. 3.3.1). This phase allows to eliminates all vacuums and bubbles embedded in the resin.

Figure 3.3.1: degassing phase of the resin employed to the manufacturing of micro and nanostructured composite samples by direct Stereo Lithography

Moreover, in order to obtain the designed uniform properties of the composite it's necessary to guarantee a uniform distribution of the particles in the matrix, during the process. Consequently, it is necessary to evaluate the time period in which the powders remains uniformly distributed. This analysis is critical also considering the long time necessary to realize by RP technology structures and elements with significant dimension.
Two test were performed. In the first experiment four samples are prepared using different quantities (see tab. 3.3.1) of graphite micro particles (glanularity< 20 μm) dispersed in the liquid resin (fig. 3.3.2).

Table 3.3.1: mixing test n° 1

Sample n°	Resin [gr]	Graphite [gr]-[% in wt]
1	10	1-10
2	10	2-20
3	10	3-30
4	10	5-50

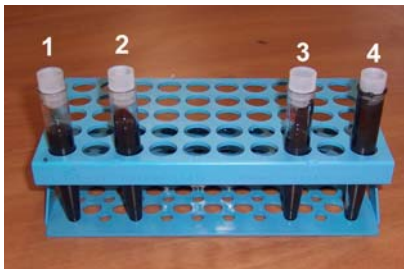

Figure 3.3.2: mixing test n° 1 & 2

After five days (fig. 3.3.3) the samples (preserved in the dark condition to avoid partial curing of the mixture) were observed. Samples **1**, and **2** showed a significant decantation of the micro powders of graphite. Instead, samples **3** and **4**, thanks to the high quantities of powders dispensed in the liquid resin, apparently showed an uniform distribution of the powders as the high concentration of the graphite cannot allow a reliable evaluation of the mixing.

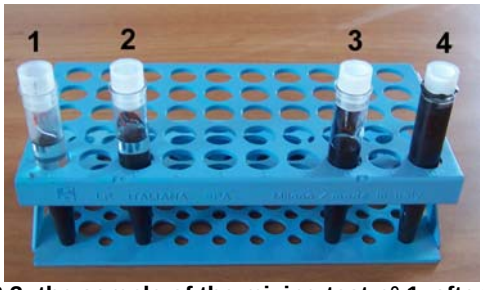

Figure 3.3.3: the sample of the mixing test n° 1, after five days

The second test has been performed with the same samples concentrations (tab. 3.3.1) but analyzing the mixing level after 3, 24 and 48 hours. As shown in the figure 3.3.4 just after 3 hours the sample with low graphite percentage (red arrow) has a partial decantation. Increasing the time this condition become more significant (fig. 3.3.5 and 3.3.6).

Figure 3.3.4: the sample of the mixing test n° 2, after 3 hours

Figure 3.3.5: the sample of the mixing test n° 2, after 24 hours

Figure 3.3.6: the sample of the mixing test n° 2, after 48 hours

These results indicate that the time useful to a direct of the RP of uniform micro and nanostructured liquid resins is very short (1 max 2 hours).
With the facility (3D System Viper SI^2 SLA System) shown in fig. 3.3.7 production tests by RP were performed. Samples are made of two different materials: 1) only resin and 2) resin + micro particles of graphite (10 % in wt). The samples (10 mm x 10 mm x 120 mm) are illustrated in fig. 3.3.8. The process time is two hours and then it is possible to hypothesize a uniform powder distribution in the polymeric matrix.
The experimental data are:

- laser power: 100 mW
- laser spot: (0.25 ± 0.025) mm
- laser wave length: 354.7 nm.

Figure 3.3.7: facility (3D System Viper SI^2 SLA System)

Figure 3.3.8: samples directly produced by RP
Left: resin + micro powders of graphite
Right: only resin

3.4 Samples characterizations (mechanical tests)

The direct RP produced samples (see previous paragraph) has been tested. Mechanical static test show that the sample with a 10% in wt of micro carbon powders has an improvement of the Young Moduls (> 12%). Besides the dynamic test show that the fracture energy (dynamic test) is the same for both samples. These results indicate that by direct RP methods it is possible to produce elements made of micro and nano - structured composite materials with significant mechanical properties. At present level of the study, these results should be considered as preliminary.

4.0 DIRECT LASER SINTERING OF METALLIC MULTIGRID AEROSPACE STRUCTURES [1]÷[11]

The "*Net Shape*" production of metallic aerospace lattice structures was experimentally studied by direct laser sintering. This method consists in a laser beam able to synthesize metallic powders. The 3D geometry of the structure is produced by the overlapping 2D cross sections of the structure itself.
Preliminary experimental tests has been performed using the facility EOSINT M250 showed in fig. 4.1.

Figure 4.1: EOSINT M250 facility

The principal characteristic of the equipment are:

- laser: CO_2
- power: 200 W
- laser spot: ~ 1 mm (in this case the minimum structure dimension is just 1 mm)
- thickness (*h*) of the single layer cured: 50 μm.

The procedure for direct laser sintering requires a 3D CAD model of the structure. The dedicated software enables the facility to produce the element sintering layer by layer (2D transversal cross section).
Fig. 4.2 illustrates an example of the direct laser sintering of a generic 2D cross section of the structure.

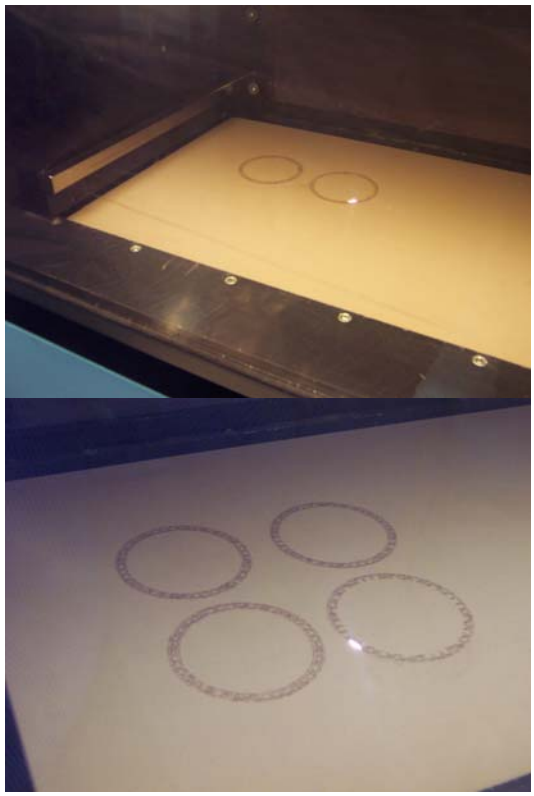

Figure 4.2: direct laser sintering of a generic 2D cross section of the designed multigrid lattice structure

The 3D CAD model of the produced "*Net Shape*" prototypes are reported in fig. 4.3 (the red elements indicates the metallic support necessary to avoid the element collapse due to the thermal deformations occurring during the synthesis process). Each prototype is constituted by ~ 1000 layers.

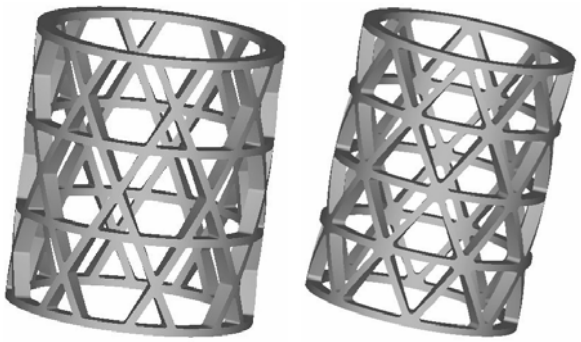

Figure 4.3: 3D CAD model of the multigrid lattice structures produced by direct laser sintering process

The dimension of the above elements are:

- diameter: external = 60 mm, internal = 52 mm
- height: 68 mm
- helical and circumferential ribs section: 4 mm x 2 mm.

Besides, the intersection of the ribs are radiused with a 2 mm radius (fig. 4.4).

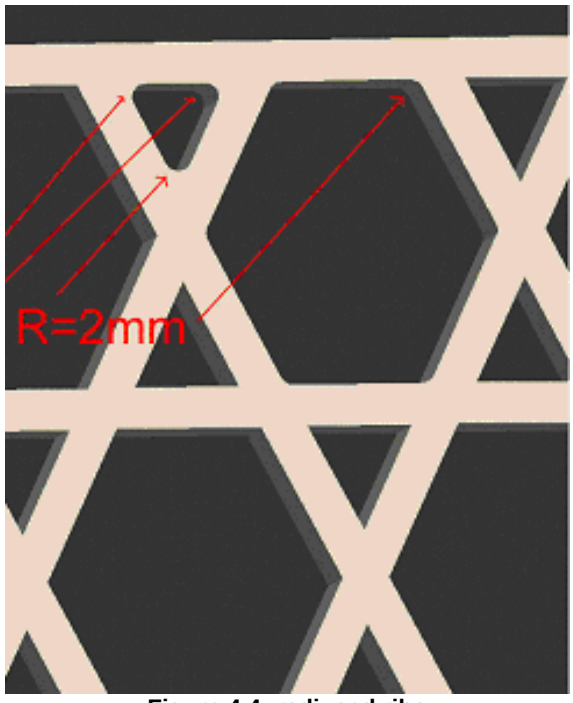

Figure 4.4: radiused ribs

The metallic powders employed is bronze alloy (the principal parameters are reported in tab. 4.1).

Table 4.1: bronze alloy powder parameters

Alloy	**Powder density**	**Powder max dimension**	**Accuracy**	**Density of the cured material**	**Relative density of the cured material**	**Traction resistance**	**Yield**	**Roughness *Rz***	**Roughness *Rz* after shoot peening**
Bronze	5.1 gr/cm^3	50 µm	± (0.07% + 50 µm)	6.3 gr/cm^3	70÷80 %	120 N/mm^2	3.3%	50 µm	1-3 µm
Thermal Expansion	**Thermal conductivity (at 23 °C)**	-	-	-	-	-	-	-	-
25E-6/K	15 W/mK	-	-	-	-	-	-	-	-

Respect the steel powders the bronze has the following characteristic:

- minor density
- minor thermal shrinkage (major dimensional stability)
- minor time process.

For preliminary test of "*Net Shape*" direct laser sintering the use of the bronze is preferable, respect to the steel, to evaluate the principal technological aspects of this methodology. The realization of simulacra in

bronze have been used essentially to test the feasibility of complex multigrid lattice structures. The study is presently directed to set up the production of similar structures made of metallic alloy suitable for aeronautic applications.

Figures 4.5÷4.6 show the produced isogrid lattice prototypes.

Figure 4.5: the produced isogrid lattice prototypes immersed in the bronze powders

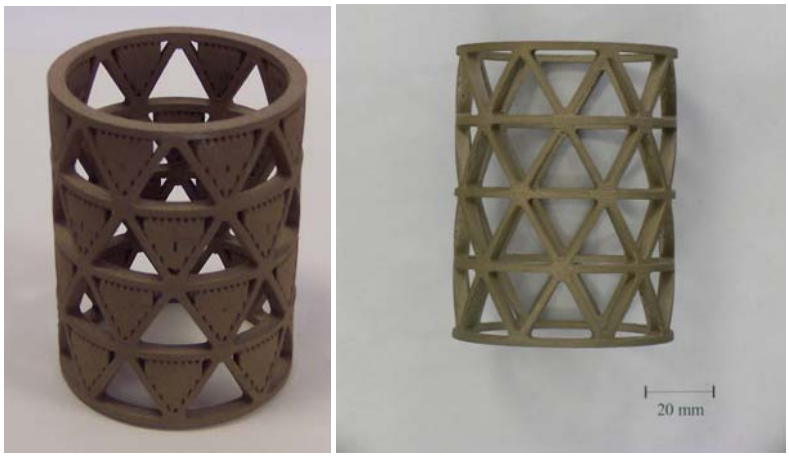

Figure 4.6: the produced isogrid lattice prototypes with the supports and after the supports removed

After the supports removal, it is necessary to improve the finishing of the structure surfaces. Typically the *shoot penning*, *sand blasting* and *ultrasound treatment* methods are used.
A sample has been cut (fig. 4.7) and analyzed by SEM to evaluate the morphology of the materials cured by laser.

Figure 4.7: sample of the prototypes employed for the SEM analysis

Fig. 4.8 shown the SEM micrographs of the sample.

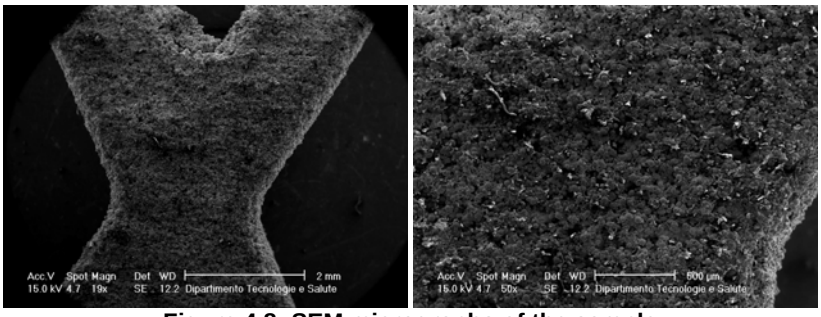

Figure 4.8: SEM micrographs of the sample

In particular in fig. 4.9 it is possible to observe:

- the material is constituted by a micro metallic particles joined together
- fused particles, single particles, and agglomerates are present
- the particles granularity is not uniform with a max dimension of ~ 50 µm (as reported in the material data sheet, see tab. 4.1).

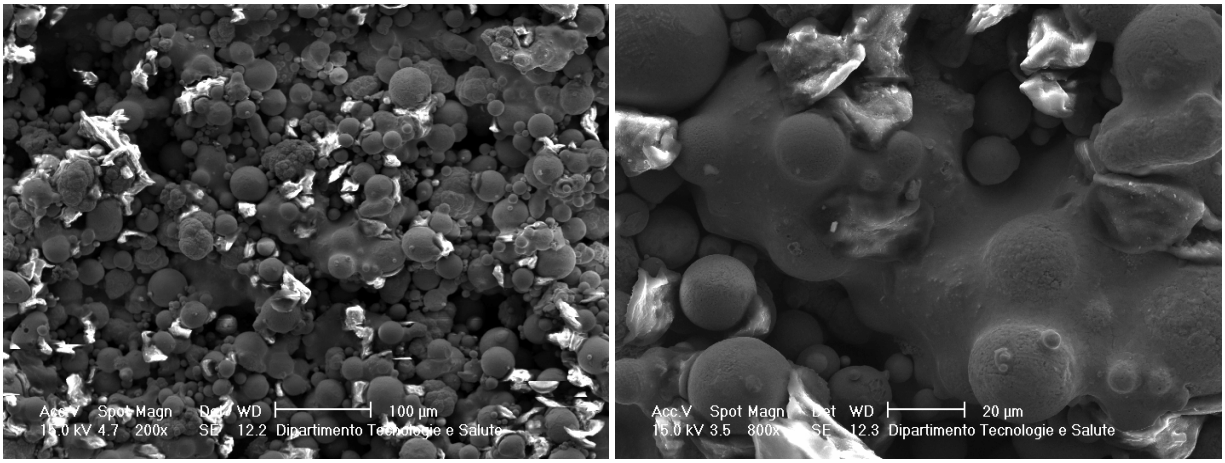

Figure 4.9: high magnification SEM micrographs of the sample

Fig. 4.10 show a further example of isogrid lattice structure (with high ribs number) produced by the method described in this paragraph.

- diameter: external = 59 mm, internal = 53 mm
- height: 68 mm
- helical and circumferential ribs section: 3 mm x 1 mm.

Figure 4.10: isogrid lattice structure sample

The SIA analysis of the bronze particles used to the direct laser sintering of the above prototypes has been performed. In tab. 4.2 the statistical data are reported. Fig. 4.11 and 4.12 illustrate, respectively, the SEM micrographs of particles and the histogram of the statistical distributions of mean particles diameter.

Table 4.2: SIA statistical analysis of the bronze particles employed to the direct laser sintering test

-	Area [μm^2]	Medium diameter [μm]	Max diameter [μm]	Min diameter [μm]	Perimeter [μm]
Medium	344,05	21,21	24,46	16,79	73,62
Max	2434,86	73,21	81,68	60,15	238,85
Min	1,39	1,61	1,85	0,68	4,61

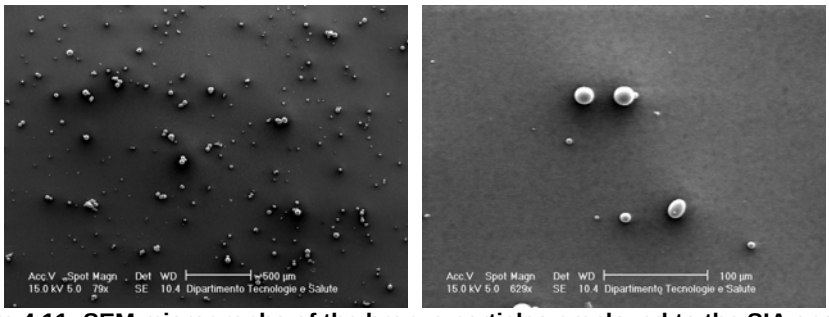

Figure 4.11: SEM micrographs of the bronze particles employed to the SIA analysis

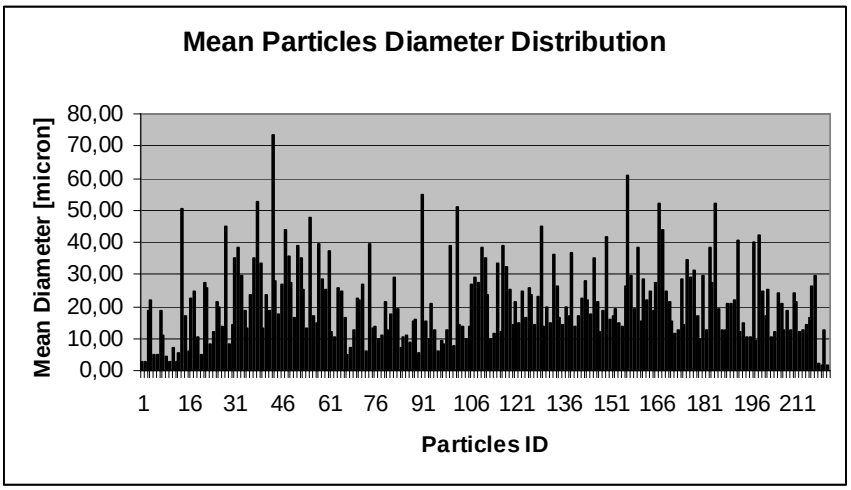

Figure 4.12: mean particles diameters distribution

To optimize the properties of the prototypes produced it is necessary to improve the surfaces finishing. In fact, considering static and periodic (fatigue) mechanical stress applied, the superficial cracks formation and propagation depends, strongly, of the surface morphology.

Using the direct laser sintering in the case of cylindrical axial symmetric structures it is preferable to growth the elements along the longitudinal direction (as performed in this paragraph, see fig. 4.5). In fact, sintering in the longitudinal direction (fig. 4.13, case **A**, see red arrow) it is possible to obtain a better final morphology of the elements. On the contrary, sintering in opposite direction (fig. 4.13, case **B**, see red arrow) the element quality decrease (fig. 4.13, case **C**, see difference between the theoretical cross section – red line, and the effective section produced with steps – black line). The steps showed in the fig. 4.13 **C**, if present, reduce significantly the properties of the structure. Then, a final cold working is requested (*shoot penning*, *sand blasting* and *ultrasound treatment*) for a significant finishing improvement.

The experimental activities indicate that the direct laser sintering method is a potential interesting technology in the manufacture of "*Net Shape*" advanced multigrid structures for aerospace applications. Of course, it is possible to realize elements for many others applications especially where the technological final requirements are less stringent, but a cost reduction is essential.

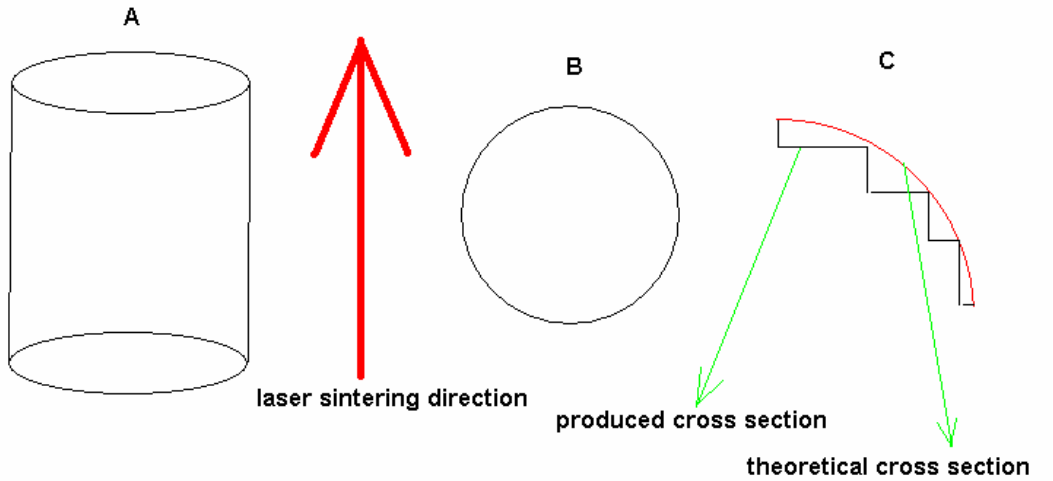

Figure 4.13: different laser sintering direction respect the structure geometry, and the relative differences in the final morphology respect the nominal shape of the element

5.0 CONCLUSIONS

In this paper the "*Net Shape*" manufacturing processes of advanced aerospace structures has been discussed. By means of the Stereo Lithography (rapid Prototyping Method) it is possible to produce positive polymeric simulacra, employed to realize flexible, and reusable, negative moulds in silicone. Finally the manufacture of composite aerospace structures (with complex shapes and respecting the as designed dimensions) is realize by Filament Winding. Moreover, by the same RP technology it is possible to manufacture a direct structural composite elements. In fact, using micro and nanoparticles addition in the polymeric matrix, various samples were directly produced and tested. The mechanical analysis shows very interesting properties. The SEM statistical analysis (SIA) of the particles embedded in the matrix it is a very significant step, because allows a complete characterization of the base materials. Moreover, different distributions of dimension and shape of the particles modify strongly the final mechanical and physical properties of the final component.
To simulate the curing processes that occurs during the RP, a specific software has been developed. With a mesh of the single cured layer, and with the Arrhenius equation, it is possible to determine the curing degree in each point of the above cured layer, in function of the process parameters (laser power, time, base materials properties and volumetric fraction, thickness, cured area, etc.). The results provided by the software are in full agreements with the experimental data and with the data sheet of the facilities used.
Direct manufacture of metallic multigrid lattice structures by means of laser sintering technology has been studied. This method provides the possibility to apply the concept of the "*Net Shape*" to lattice metallic structures for aerospace applications.
For each method described in this paper, it is possible to produce elements with any complex shape and geometry. A significant improvement in the quality of the prototypes produced can be obtained if the "*Net Shape*" processes utilized is correctly used and optimized.
The addition of micro and nano powders represent a possible means to improve the final properties of the "*Net Shape*" manufactured structures.

6.0 ACKNOWLEDGMENTS

Thanks to Mr. *Luca Innocenzi* (CSM Centro Sviluppo Materiali S.p.A., Italy) for the collaboration in the direct laser sintering of the samples.

Special Thanks to Dr. *Mario Sarasso* (SISTEMA COMPOSITI S.p.A., Italy) for the collaboration in the manufacturing of the cylindrical anisogrid lattice prototypes (see figure 2.2.3÷2.2.4).

Thanks to Dr. *Luigi Paoletti* and Dr. *Biagio Bruni* (ISS – Istituto Superiore di Sanità – Dipartimento di Tecnologie e Salute – Roma) for the collaboration in the nanoparticles and SEM, SIA and EDX characterizations of the nanoparticles and of the direct laser synthesized samples.

7.0 BIBLIOGRAPHY

[1] P. Jacobs "*Stereo Lithography and other rapid prototyping and manufacturing technologies*", Society of Manufacturing Engineers, Dearbom, MI, 1996

[2] F. Erzincanh, M. Ermurat "*Comparison of the direct metal laser fabrication technologies*", Gebze Institute of Technology, Design and Manufacturing

[3] K. Kuzman, B. Nardin "*Determination of manufacturing technologies in mould manufacturing*", TECOS, Slovenian Tool and Die Development Centre, Mariborska 2, SI-3000 Celje, Slovenia

[4] P. F. Jacob, "*Recent advances in rapid tooling from Stereo Lithography*", Proceedings of the Seventh International ICRP Conference, California, USA, 9–12 March 1997, pp. 338–354

[5] P. Rahmati, S. Dickens "*Stereo Lithography* for Injection mould tooling", Rapid Prototyping Journal, v. 3, n0 2, pp. 53-60, 1997

[6] S. Menge, G. Mohren, G. Michaeli "*How to Make injection molds*", Ed. Hanser 2003

[7] M.C. Donald "*Engineers Guide to composite materials*", 1990

[8] Y. Tang "*Stereo Lithography cure process modeling*", A Dissertation Presented to The Academic Faculty - Georgia Institute of Technology - August 2005

[9] A. Simchi, H. Pohl "*Direct laser sintering of iron – graphite powder mixture*", Materials Science and Engineering A 383 (2004) 191–200, January 2004

[10] A. Simchi, H. Pohl "*Effects of laser sintering processing parameters on the microstructure and densification of iron powder*", Mater. Sci. Eng. A359 (2003) 119

[11] J. P. Kruth, L. Froyenb, J. Van Vaerenbergh, P. Mercelis, M. Rombouts, B. Lauwers "*Selective laser melting of iron – based powder*", Journal of Materials Processing Technology 149 (2004) 616–622

[12] M. Regi, F. Mancia, M. Marchetti "*Design and characterization of anisogrid lattice structures with carbon nanotubes*", Proceedings International Workshop on MEMS and Nanotechnology Integration (MNI): Application, 10 - 11 Maggio 2004, Montreux (Svizzera)

[13] M. Regi, M. Marchetti, F. Mancia, G. Allegri "*Synthesis of carbon nanotubes and their application in "anisogrid lattice structures"*, Proceedings SEM X International Congress & Exposition on Experimental and Applied Mechanics, 5th International Symposium on MEMS and Nanotechnology, June 7 -10 2004 Costa Mesa California USA

[14] M. Regi, F. Mancia "*Synthesis and characterization of carbon-nanotubes and their application in the aerospace engineering*", Proceedings Polymer Fibers 2004 14-16 July 2004 UMIST Conference Centre Manchester UK

[15] M. Regi, F. Mancia, M. Marchetti, G. Totaro, F. De Nicola, V. V. Vasiliev, A. F. Rasin "*Nanostructured composite materials and anisogrid lattice structures for aerospace applications, Part A: synthesis of carbon nanotubes and their application in anisogrid lattice structures", Part B: optimezed design of isogrid and anisogrid lattice structures*", Proceedings 55th IAC International Astronautical Congress IAF, October 4 - 8 2004 Vancouver Canada

[16] M. Marchetti, M. Regi, F. Mancia "*Damage response of anisogrid lattice aerospace structures*", Proceedings dell'ICOSAAR2005 9th International Conference on Structural Safety and Reliability Rome, Italy, June 19 – 23 2005

MEETING DISCUSSION – PAPER NO: 20

Author: M. Regi

Discusser: X. Wu

Question: What is the feedstock of nano materials?

Response: It is resin.

Discusser: P. Brown

Question: What applications would your lattice structures be used for?

Response: The possible aerospace applications are: aircraft fuselages, launchers, and flat panels for satellite parts

Discusser: J. Savoie

Question: What is the porosity of material (metallic) after direct laser sintering? Which materials were investigated?

Response: The porosity is under investigation. It is necessary to improve this parameter to optimize the mechanical properties of the elements produced. Bronze and steel alloy have been investigated.

Centro Sviluppo Materiali S.p.A.

La Sapienza
Università degli Studi di Roma

DEPARTMENT OF AEROSPACE AND ASTRONAUTIC ENGINEERING
SCHOOL OF AEROSPACE ENGINEERING

Develop of 3D Advanced Rapid Prototyping

Multipurpose Structures with Micro and Nano Materials

F. Mancia, M. Marchetti, M. Regi, S. Lionetti
A. Marranzini, F. Mazza, P. Coluzzi

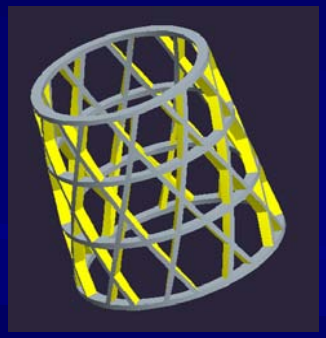

R&T ORGANIZATION

AVT 139
Specialists' Meeting on
Cost Effective Manufacture via Net Shape Processing

Amsterdam – The Nederland, May 15 – 19 2005

RP MANUFACTURING OF MULTIGRID LATTICE STRUCTURES

FLAT AND CYLINDRICAL PROTOTYPE REALIZATION

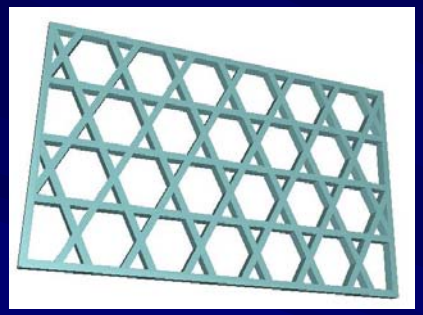

CAD MODEL

RAPID PROTOTYPING

SILICONE NEGATIVE MOULD

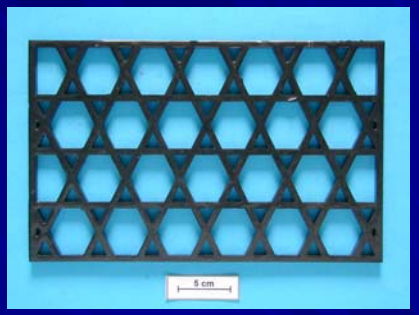

FLAT PROTOTYPE

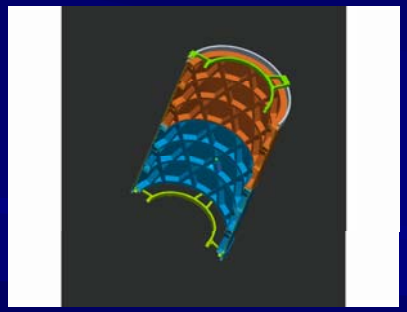

CAD MODEL

POSITIVE MOULD

SILICONE NEGATIVE MOULD

MANDREL FOR THE PROTOTYPE PRODUCTION USING THE FILAMENT WINDING

RP MANUFACTURING OF MULTIGRID LATTICE STRUCTURES

FLAT AND CYLINDRICAL PROTOTYPE REALIZATION

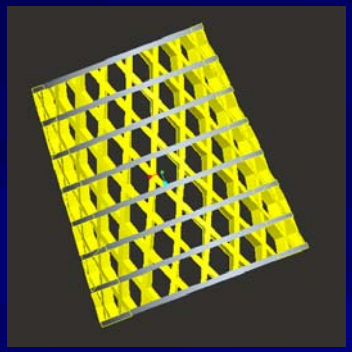
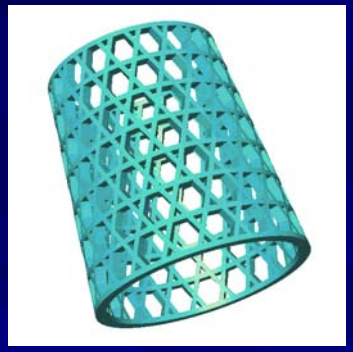
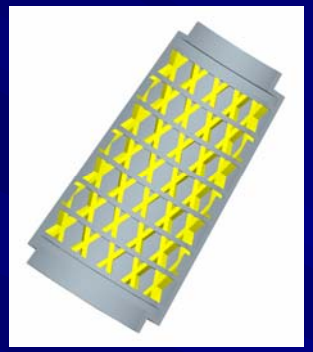


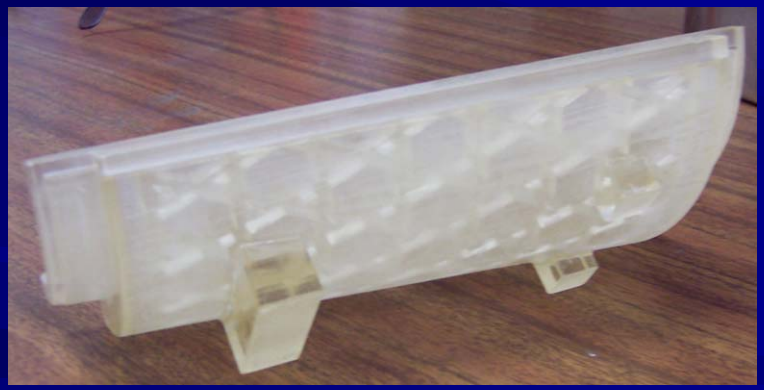
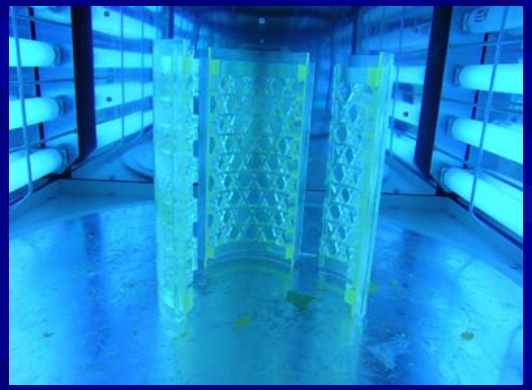


RP MANUFACTURING OF MULTIGRID LATTICE STRUCTURES

FEM ANALYSIS

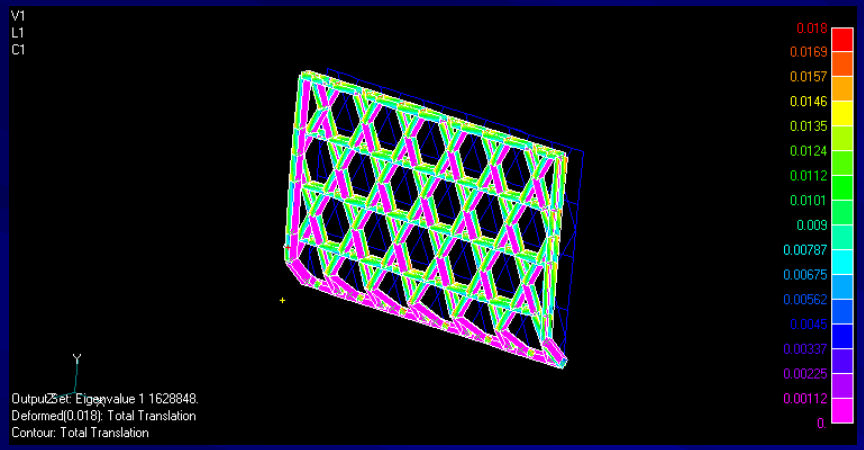

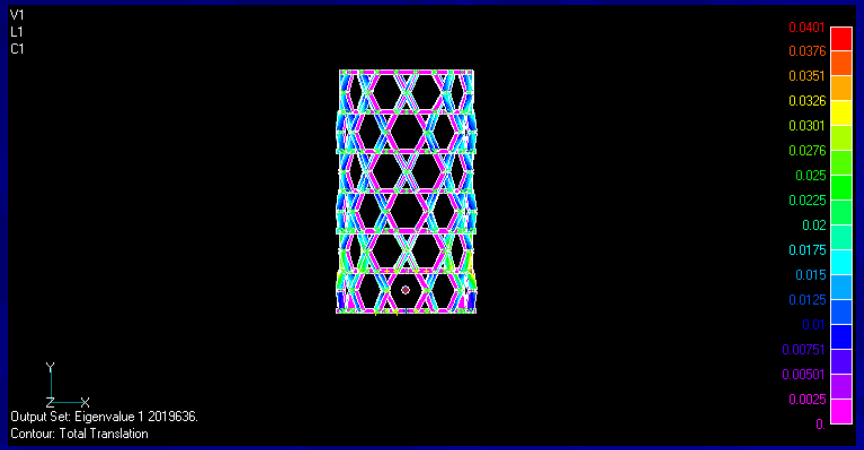

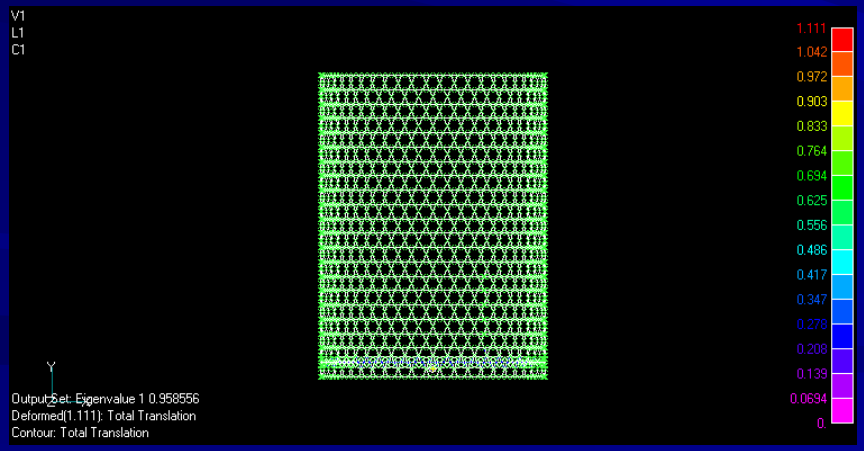

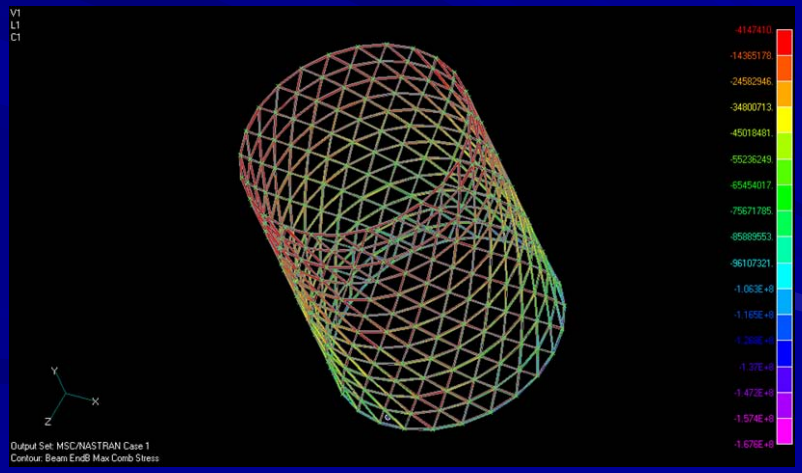

RP MANUFACTURING OF MULTIGRID LATTICE STRUCTURES

FLAT AND CYLINDRICAL PROTOTYPE REALIZATION

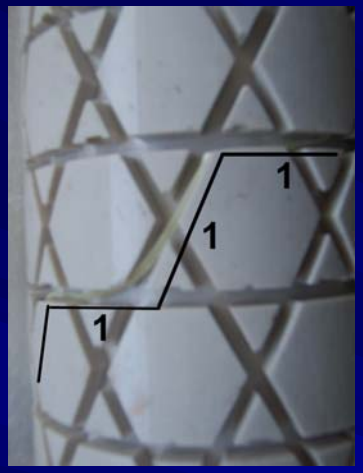

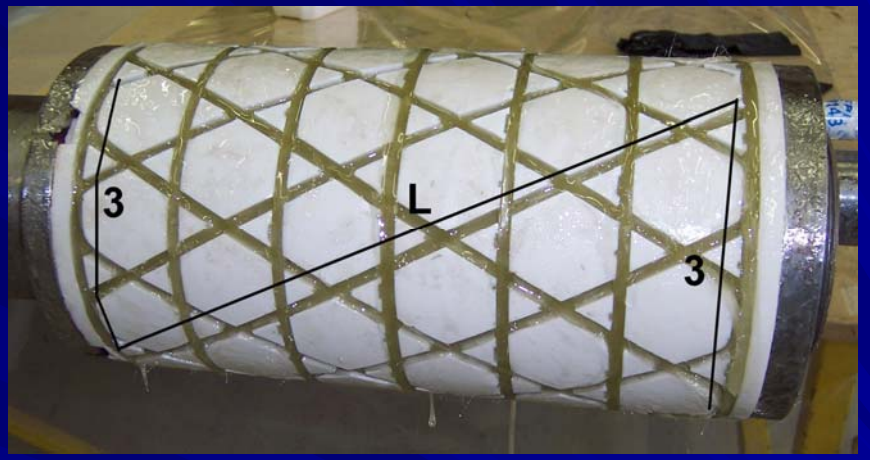

RP MANUFACTURING OF MULTIGRID LATTICE STRUCTURES

FLAT AND CYLINDRICAL PROTOTYPE REALIZATION

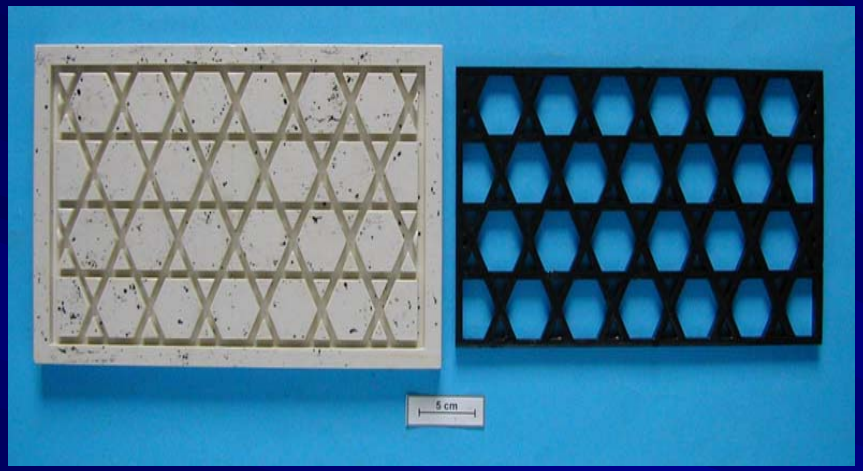

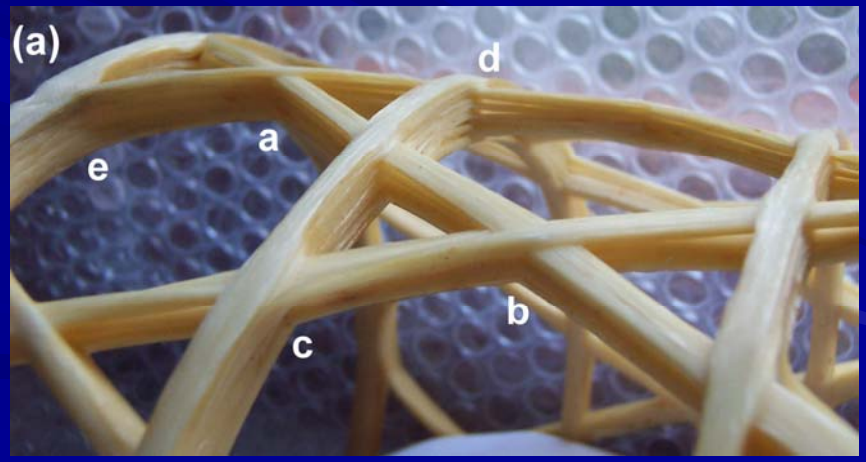

RP MANUFACTURING OF MULTIGRID LATTICE STRUCTURES

MECHANICAL TEST

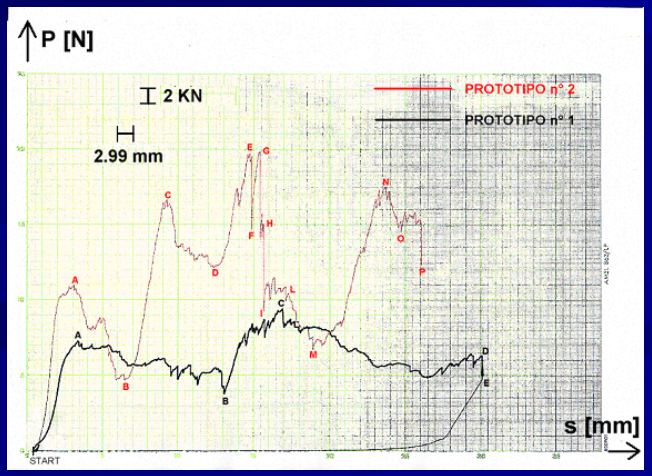

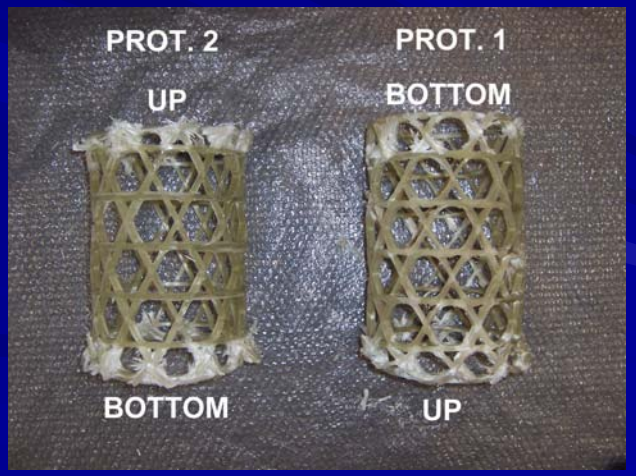

RP AND STEREOLITHOGRAPHY

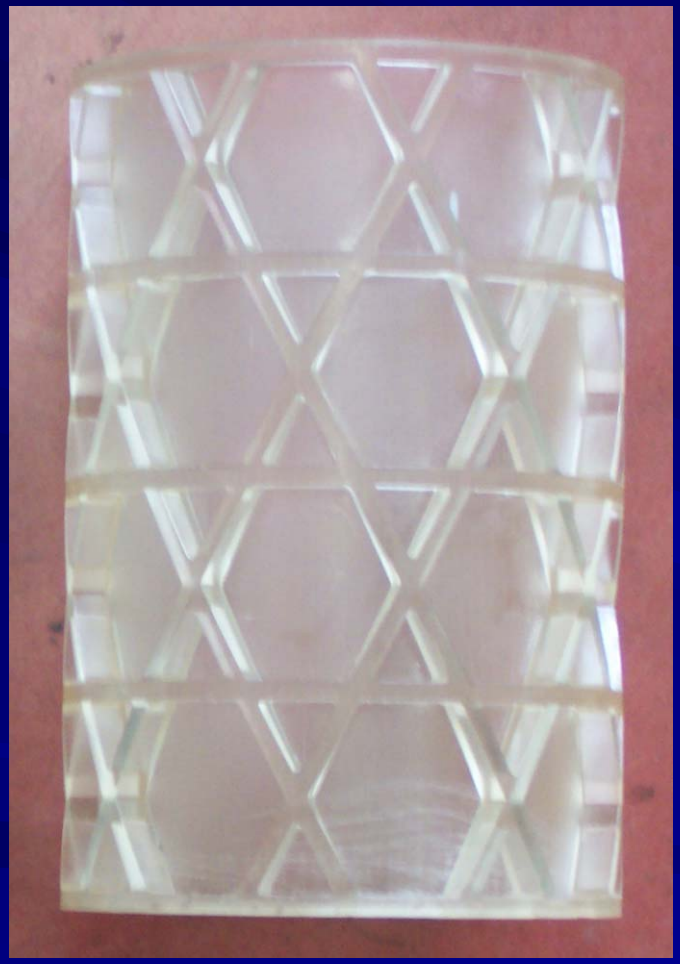

SYNTHESIS OF CARBON NANOTUBES

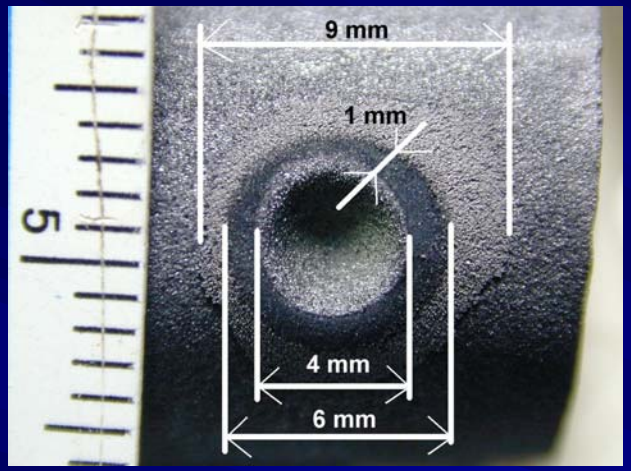

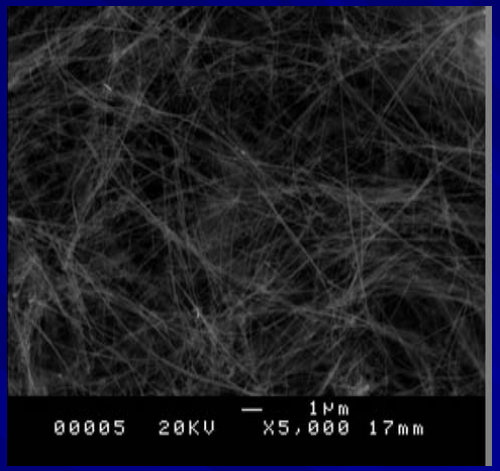

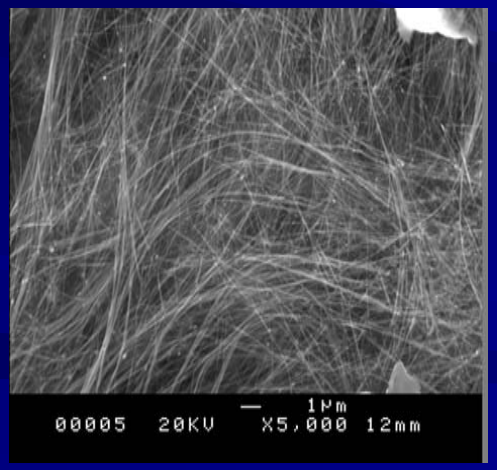

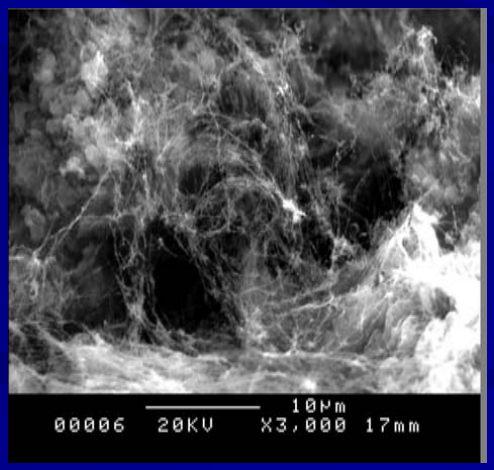

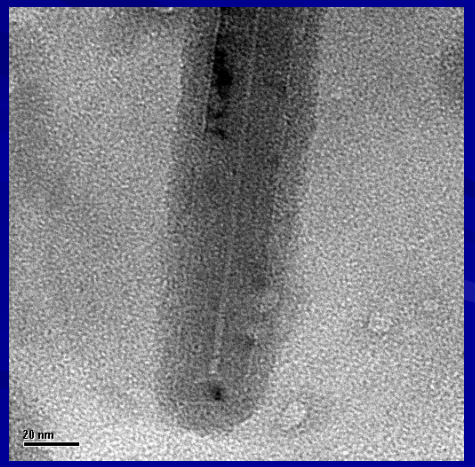

CARBON NANOTUBES MORPHOLOGICAL ANALYSIS

CATHODE ELECTRODE SURFACE
AFTER THE ARC DISCHARGE
(OPTICAL MICROSCOPY ANALYSIS)

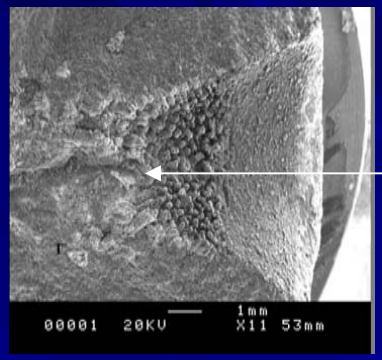

LONGITUDINAL
ANALYSIS

MORPHOLOGICAL STUDIES OF
THE GRAPHITE ELECTRODE SURFACE
TO DIFFERENT LEVELS OF ARC RADIAL PENETRATION
(SEM PHOTO)

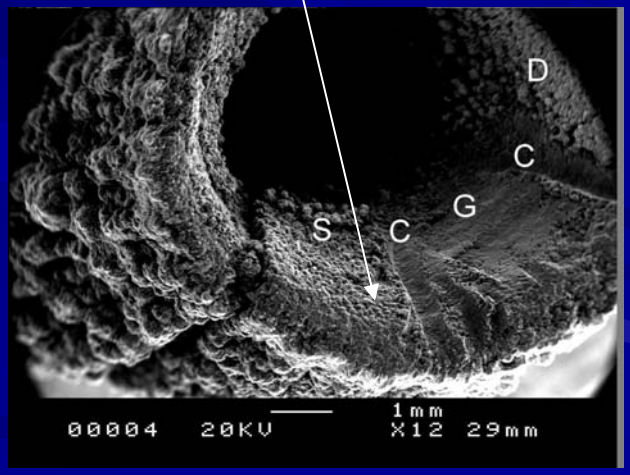

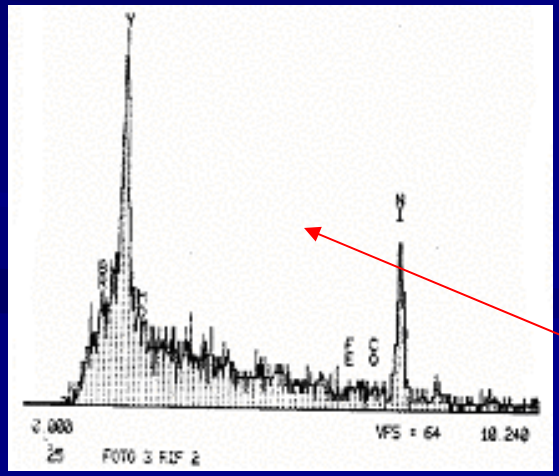

EDX ANALYSIS TO DETERMINE THE CHEMICAL
CHARACTERIZATION OF THE CHATODE ELECTRODE
(CARBON, NICKEL, ITTRIUM, COBALT)

AFM CHARACTERIZATIONS

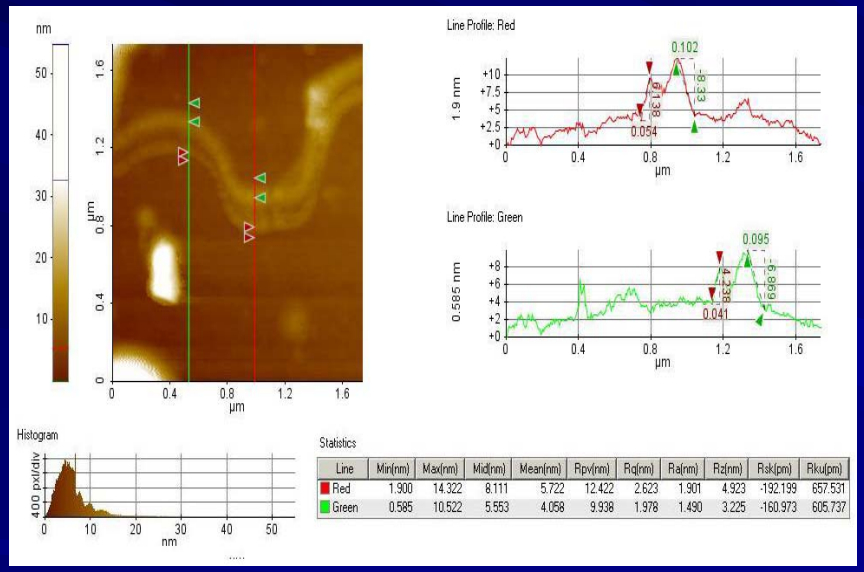

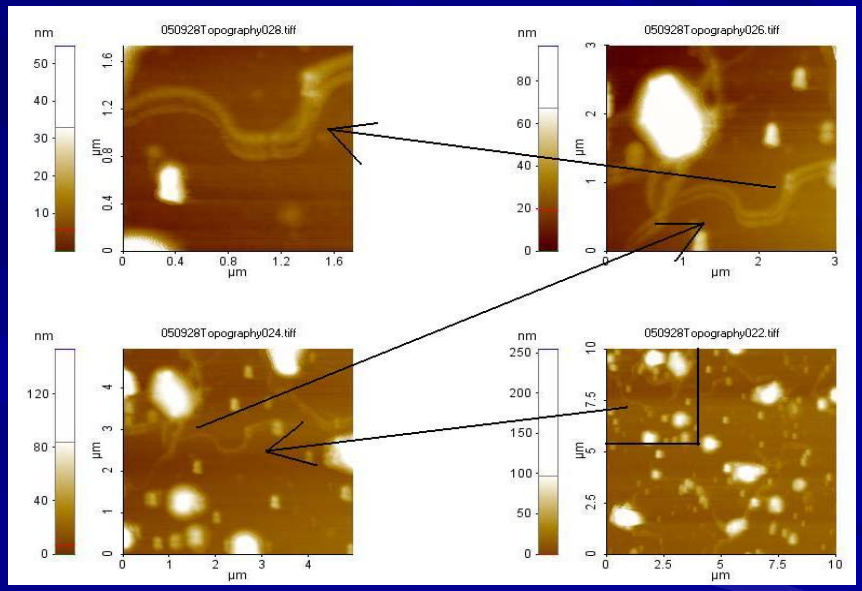

NUMERICAL MODEL OF DIRECT RP CURING PROCESS

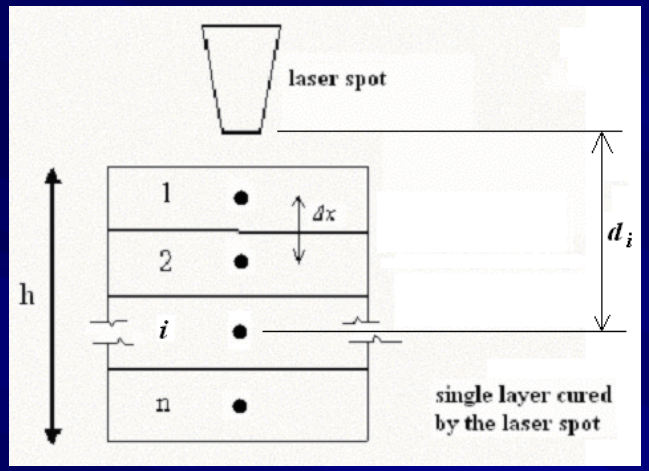

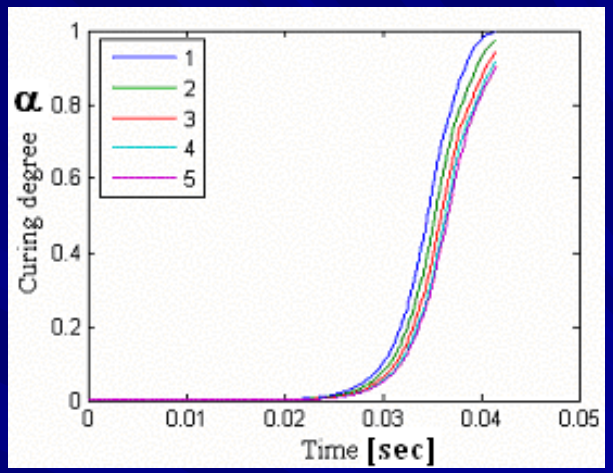

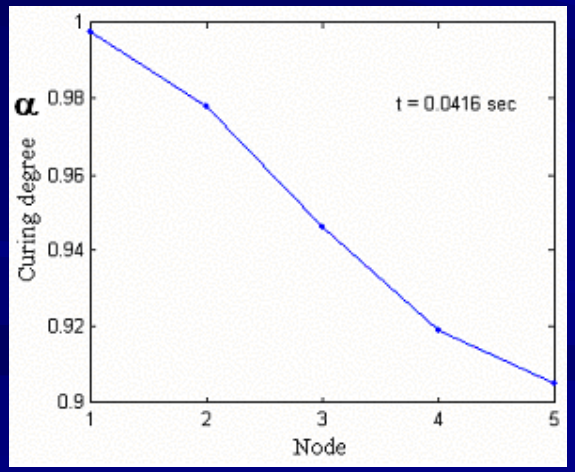

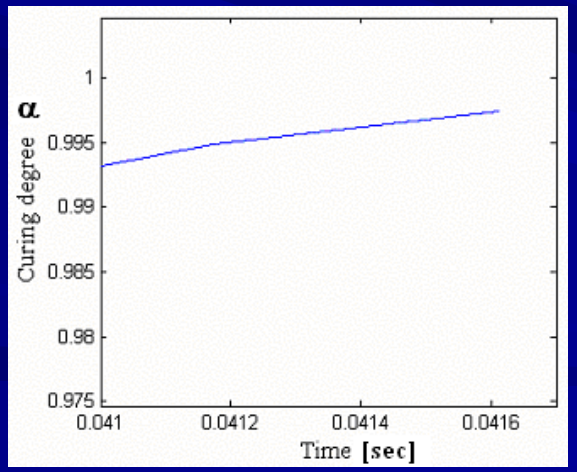

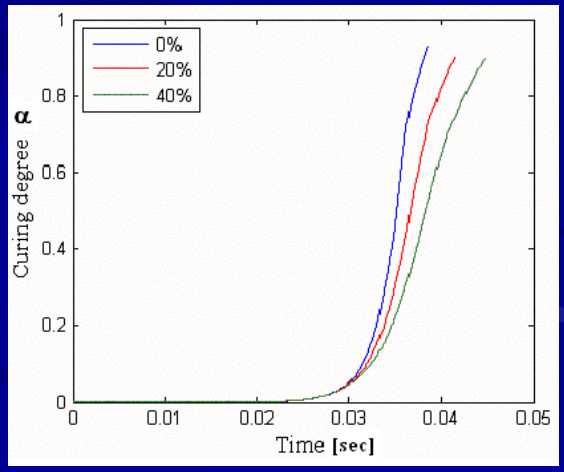

SEM ANALYSIS OF THE MICRO POWDERS ADDED IN THE POLYMERIC MATRIX

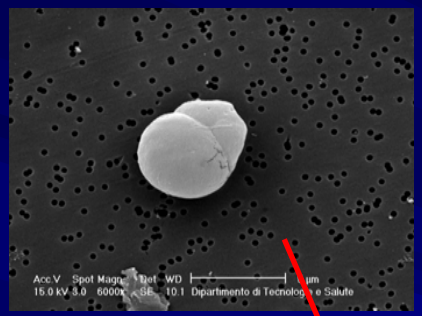

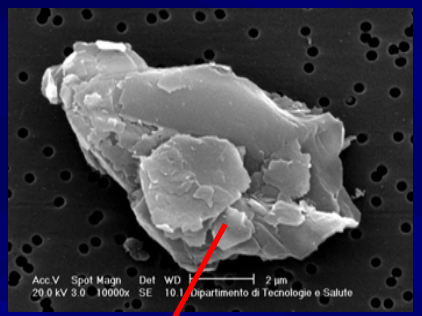

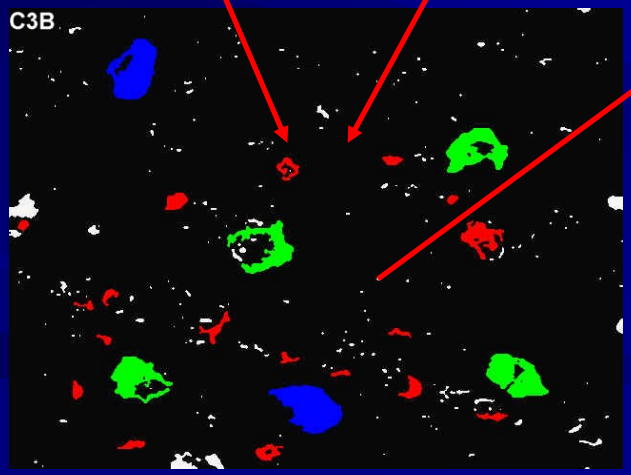

	ID Particle	ID Class	Area µm²	Diameter Mean µm	Diameter Max µm	Diameter Min µm	Perimeter µm
SAMPLE n° 1 (fig. 3.8 left)							
	1	3	8,11	3,77	4,25	3,08	15,98
	2	2	6,73	3,83	4,19	3,12	17,71
	3	1	0,60	1,14	1,38	0,65	3,17
	4	1	1,00	1,47	1,63	1,32	7,97
	5	1	1,20	1,42	1,57	1,10	4,25
	6	1	0,32	0,68	0,74	0,61	2,05
	7	1	0,35	0,71	0,78	0,67	2,19
	8	2	5,48	4,08	4,45	3,15	21,60
	9	1	3,22	2,66	2,88	2,36	14,44
	10	1	0,53	1,08	1,16	0,84	3,84
	11	1	0,33	1,15	1,37	0,62	3,47
	12	1	1,07	2,12	2,34	1,53	7,38
	13	1	0,39	1,33	1,57	0,58	3,67
	4	1	0,33	0,92	1,08	0,57	2,68
	15	1	0,42	1,12	1,26	0,75	3,61
	16	2	6,98	3,75	4,42	2,48	16,15
	17	2	6,01	3,58	4,08	2,83	19,00
	18	1	0,33	1,13	1,30	0,53	2,91
	19	1	1,13	1,52	1,59	1,46	5,10
	20	1	0,59	1,09	1,26	0,71	3,13
	21	3	9,10	4,26	5,08	2,99	13,66
	22	1	0,62	1,75	2,05	0,62	4,62
	23	1	0,64	1,59	1,81	0,61	4,09
	24	1	1,10	1,55	1,80	1,12	6,38
mean			**2,36**	**1,99**	**2,25**	**1,43**	**7,88**
max			**9,10**	**4,26**	**5,08**	**3,15**	**21,60**
min			**0,32**	**0,68**	**0,74**	**0,53**	**2,05**
SAMPLE n° 2 (fig. 3.8 right)							
	1	1	3,75	3,61	4,35	1,91	10,87
	2	1	0,32	0,99	1,10	0,75	3,29
	3	1	0,32	0,94	1,14	0,42	2,50
	4	3	11,33	4,42	4,55	4,14	14,48
	5	1	1,73	1,66	1,89	1,39	5,91
	6	1	2,64	2,09	2,47	1,60	6,89
	7	1	0,80	1,09	1,26	0,86	3,41
	8	1	2,75	2,42	2,92	1,67	7,49
	9	3	9,56	4,22	4,90	3,25	15,74
	10	1	0,31	0,76	0,88	0,53	2,31
	11	1	1,18	1,35	1,47	1,03	4,19
	12	1	0,31	0,89	1,06	0,50	2,48
	13	1	1,12	1,86	2,11	1,44	7,25
	14	2	6,54	4,25	4,51	2,94	20,41
	15	1	0,85	1,41	1,59	1,16	5,27
	16	3	8,41	5,97	6,86	3,04	24,61
mean			**3,24**	**2,37**	**2,69**	**1,66**	**8,57**
max			**11,33**	**5,97**	**6,86**	**4,14**	**24,61**
min			**0,31**	**0,76**	**0,88**	**0,42**	**2,31**

MIXING TEST AND DIRECT RP OF MICRO AND NANO STRUCTURED POLYMERIC SAMPLES

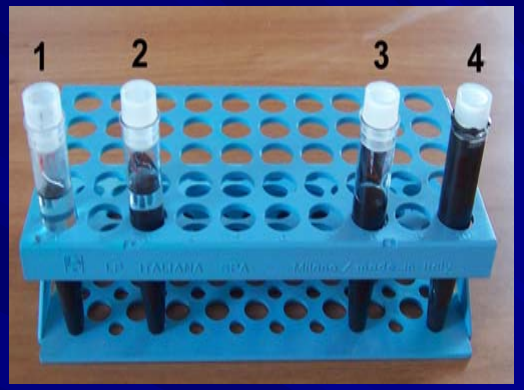

DIRECT LASER SINTERING OF METALLIC MULTIGRID LATTICE AEROSPACE STRUCTURES

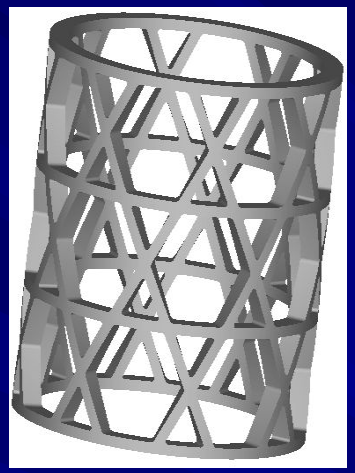

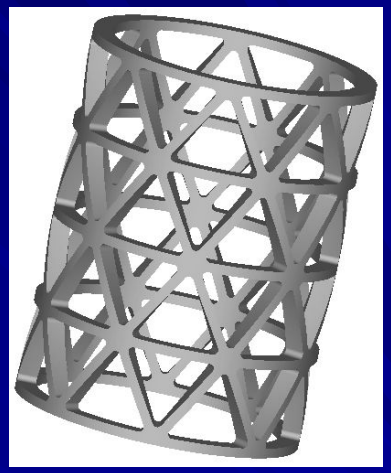

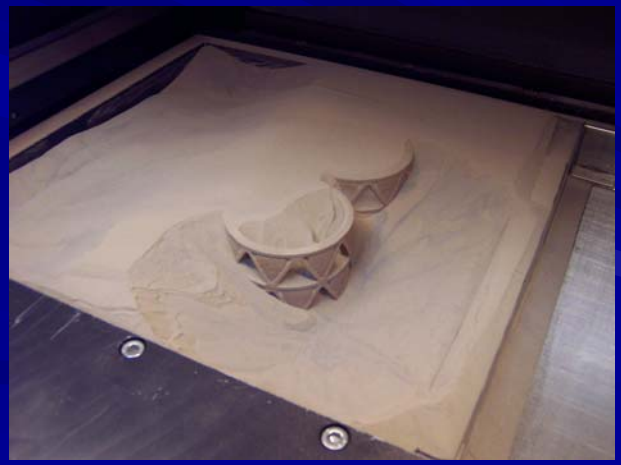

SEM ANALYSIS OF THE METALLIC MICRO POWDERS

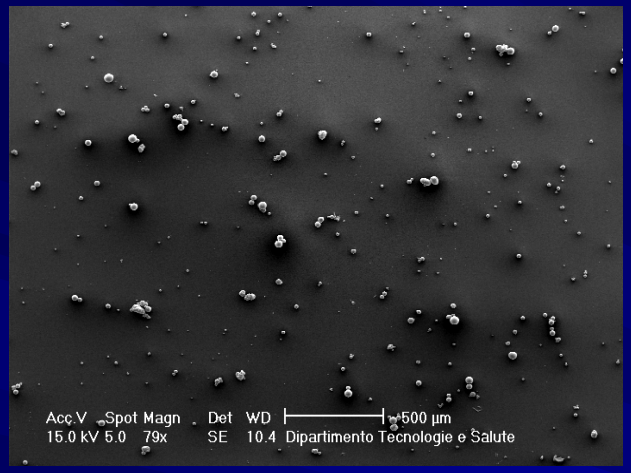

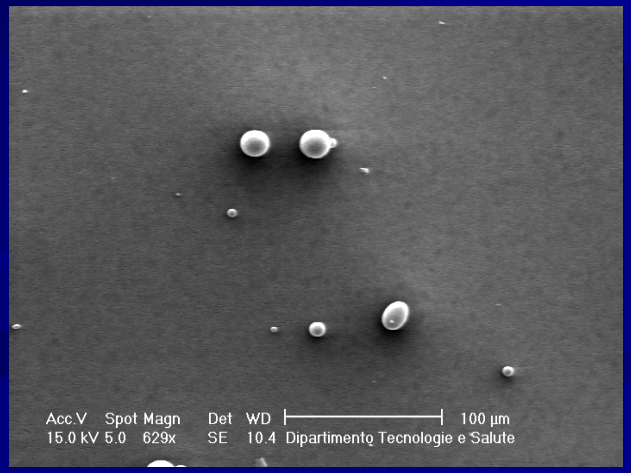

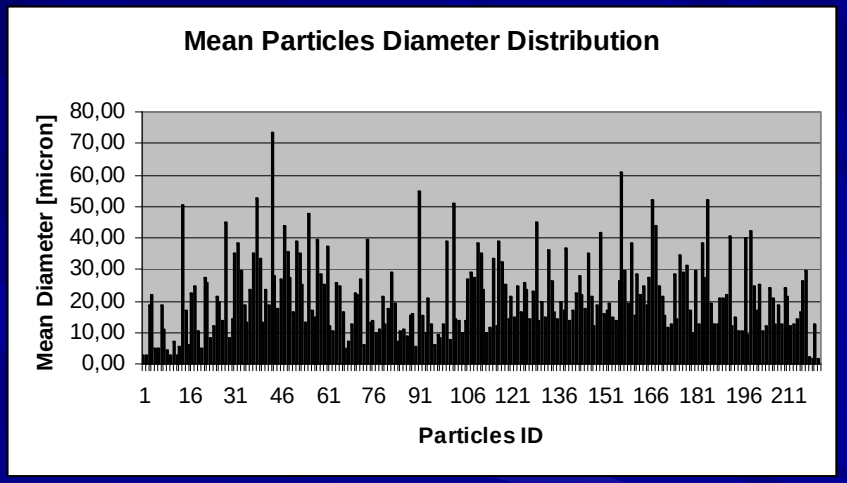

DIRECT LASER SINTERING OF METALLIC MULTIGRID LATTICE AEROSPACE STRUCTURES

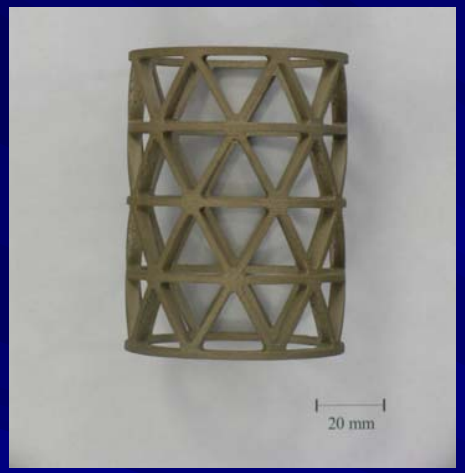

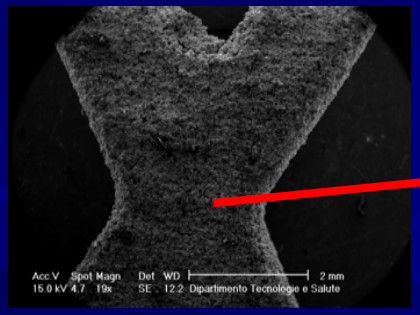

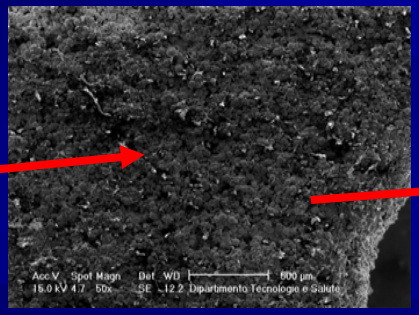

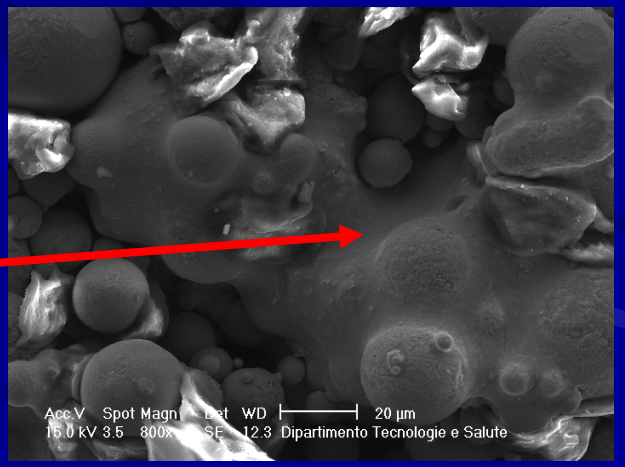

DIRECT LASER SINTERING OF METALLIC MULTIGRID LATTICE AEROSPACE STRUCTURES

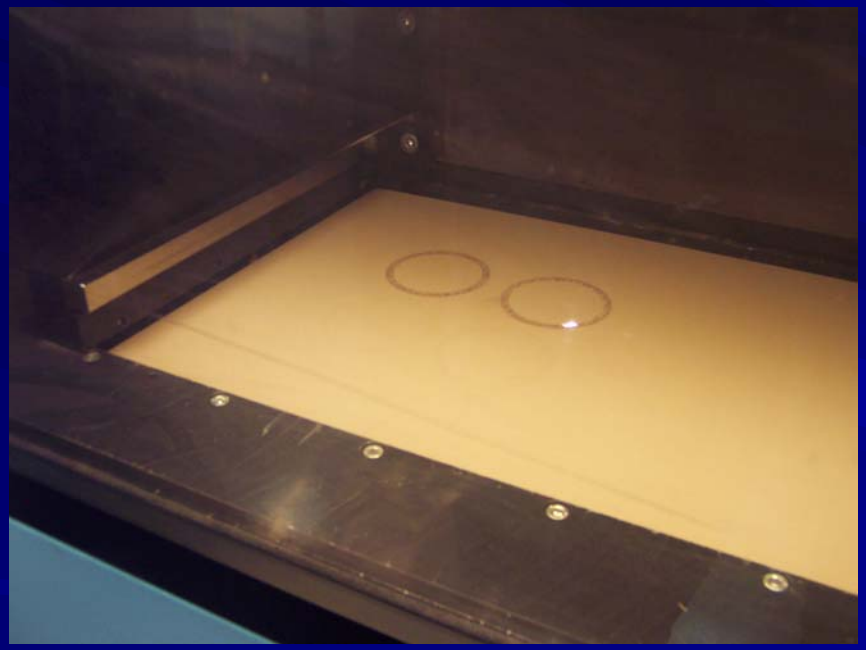

CONCLUSIONS

- Net Shape manufacturing process of advanced multigrid aerospace lattice structures
- Manufacturing of silicone negative mould
- RP curing process simulation by software
- Direct RP manufacturing of micro and nano structured polymeric composite materials
- Direct Laser Sintering of metallic multigrid aerospace lattice structures.